CHAPTER FOUR

RESULTS AND DISCUSSION

4.0 Introduction

The main objective of this research project was to study blends of PHB/PVAc and their thermal stability and biodegradability. It also includes studying some parameters affecting the rheology of these blended solutions to study compatibility. The blended thin films of PHB/PVAc are characterized by employing FTIR, SEM, thermal studies and biodegradable property.

4.1 Viscosity Measurement

4.1.1 Rheological study of PHB/PVAc blended solutions

All samples of PHB and PVAc solutions were prepared by dissolving polymer in chloroform. In this study, the effect of viscosity on the shear rate and shear stress on shear rate of PHB/PVAc blended solutions was studied. The shear rate dependent viscosity of PHB/PVAc blended solutions as a function of shear rate at 25 °C are shown in **Figures (4.1- 4.2)**. Higher temperatures were not applied to avoid thermal degradation of the polymers and solvent evaporation while lower temperature could not be applied due to the PVAc formation in some PHB/PVAc blended solutions. The behaviour of the viscosity-temperature relationship for the blends showed a decrease in viscosity with increase in the shear rate, which is typical for many polymers. Also, Newtonian behaviour (in which the relation between the shear or apparent viscosity and the shear rate is linear) was observed at temperatures for ratios of 100/0, 0/100, 90/10, 85/15, 80/20, 75/25, 70/30 and 65/35.

In rheology the melt index and the viscosity using capillary viscometer or a rotational rheometer were measured. Rheology is most often used for materials in the liquid state and the material flow. Polymer melts are characterized by a viscosity which depends on the shear rate (Park *et al.*, 2001).

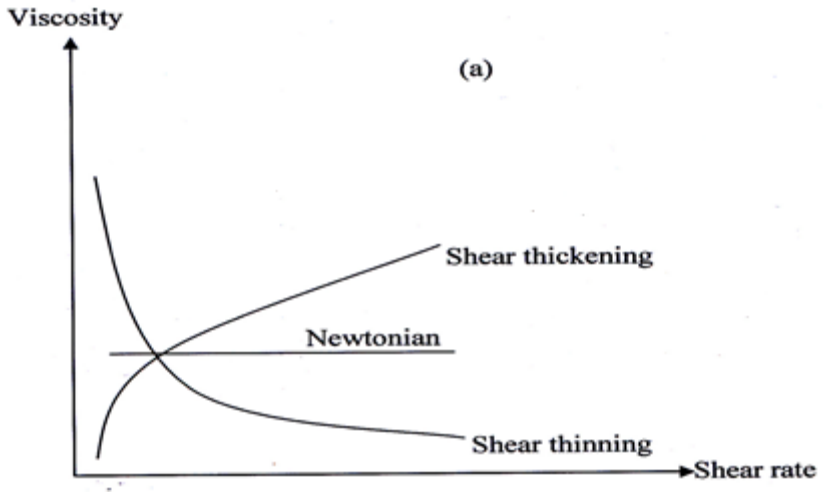

Figure (4.1): The relationship between viscosity and shear rate for time independent flow fluids (Guest *et al.*, 2013).

Viscosity increases with increasing shear rate for the blended solutions. In addition, the increases in shear stress with increasing shear rate were found to be more remarkable at high viscosity. The PHB/PVAc blended solutions exhibited similar behavior and no significant change was observed with excepting the ratio 90/10, 85/15 (Figure (4.2.d, f)) whereby increasing at a shear rate led to a decrease in viscosity (Park *et al.*, 2001; El-Hefian *et al.*, 2010). The decrease is attributed to the dilution shear stress effect of the PVAc polymer, eventually resulting in a low shear viscosity. This rheological behavior of the PHB/PVAc polymer blend was found to be similar to results (Khanna & Srivastava, 2005). Influence of PP content on the polyfluorinated ethylene propylene (FEP)/ polypropylene (PP) blend shear viscosity also shows the relationship between the shear stress and the shear rate (Nikolova & Schnabel, 2014) while the rheological behavior of the PHB and PEO solutions as well as their mixtures exhibit non-Newtonian (shear thinning) behavior which is described by the Ostwald-de Waele model.

(a)

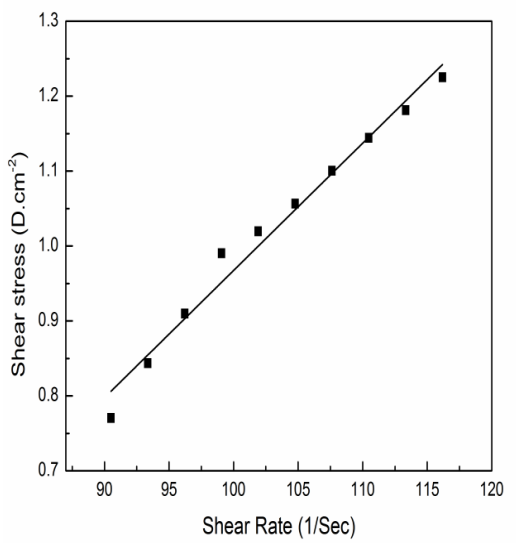
Shear stress (D.cm^{-2})
Shear Rate (1/Sec)

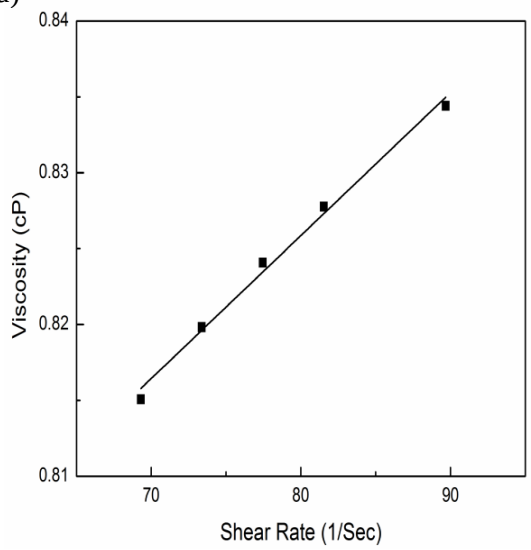
Viscosity (cP)
Shear Rate (1/Sec)

(b)

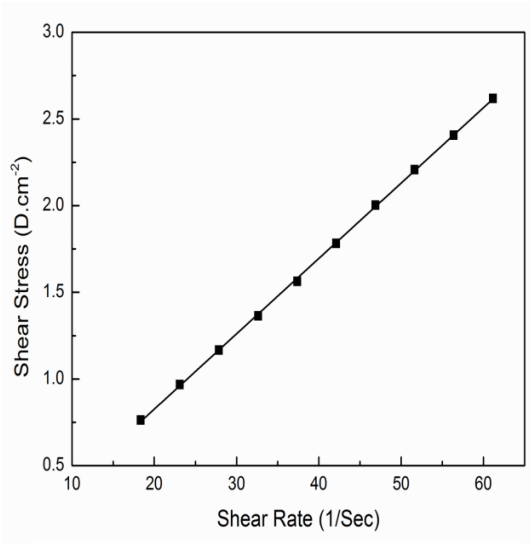
Shear Stress (D.cm^{-2})
Shear Rate (1/Sec)

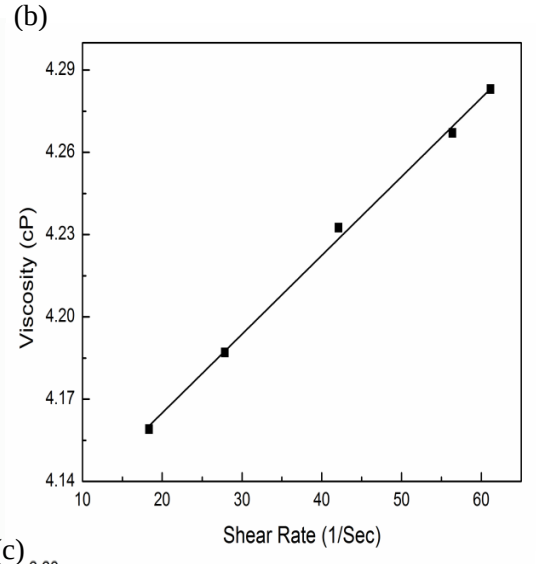
Viscosity (cP)
Shear Rate (1/Sec)

(c)

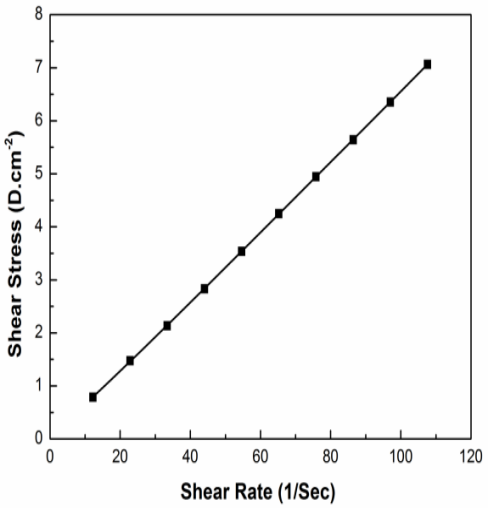
Shear Stress (D.cm^{-2})
Shear Rate (1/Sec)

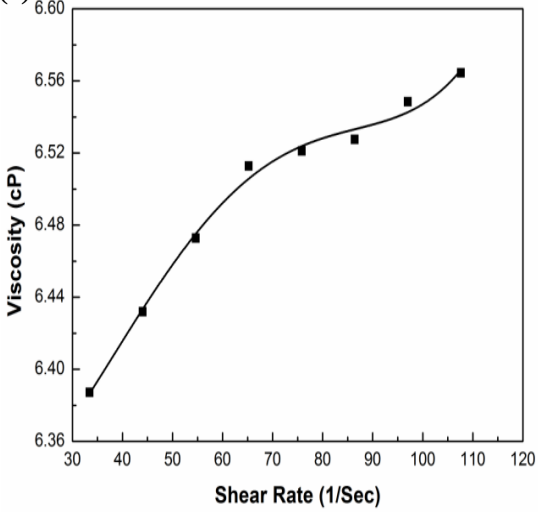
Viscosity (cP)
Shear Rate (1/Sec)

(d)

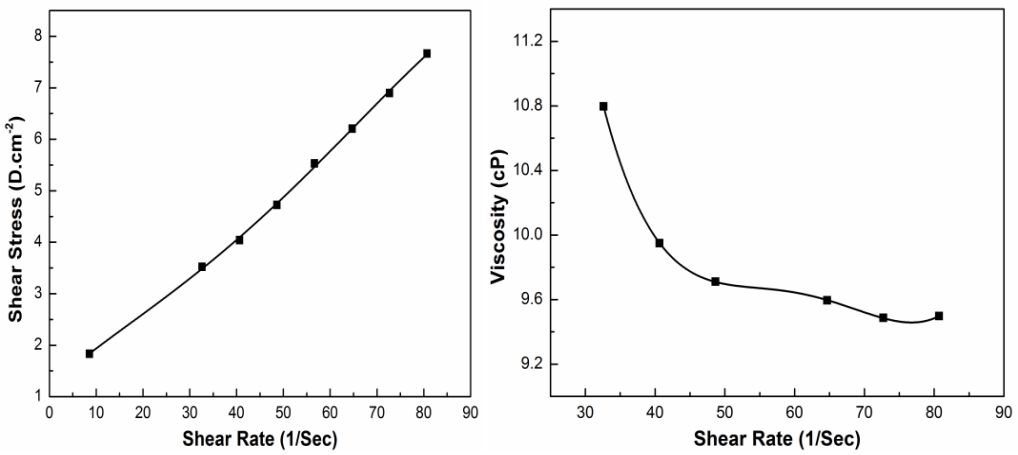
Shear Stress (D.cm-2)
Shear Rate (1/Sec)
Viscosity (cP)
Shear Rate (1/Sec)

(e)

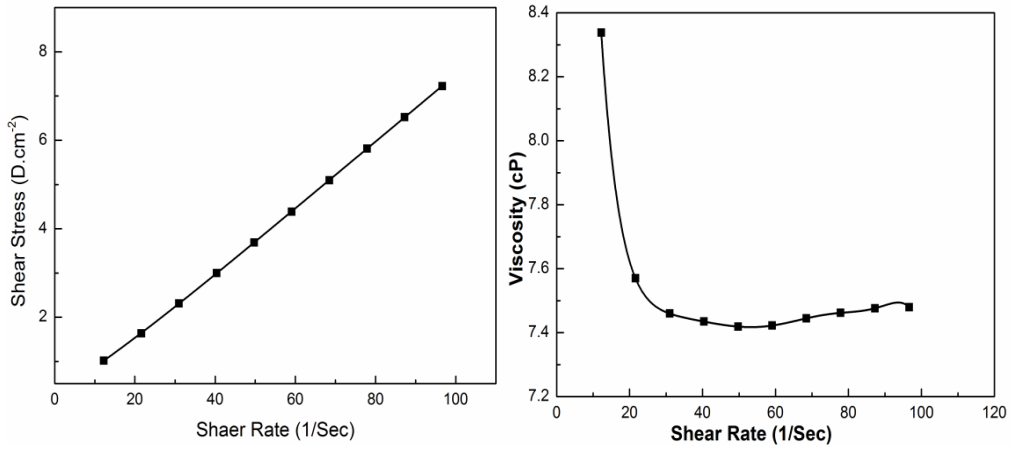
Shear Stress (D.cm-2)
Shaer Rate (1/Sec)
Viscosity (cP)
Shear Rate (1/Sec)

(f)

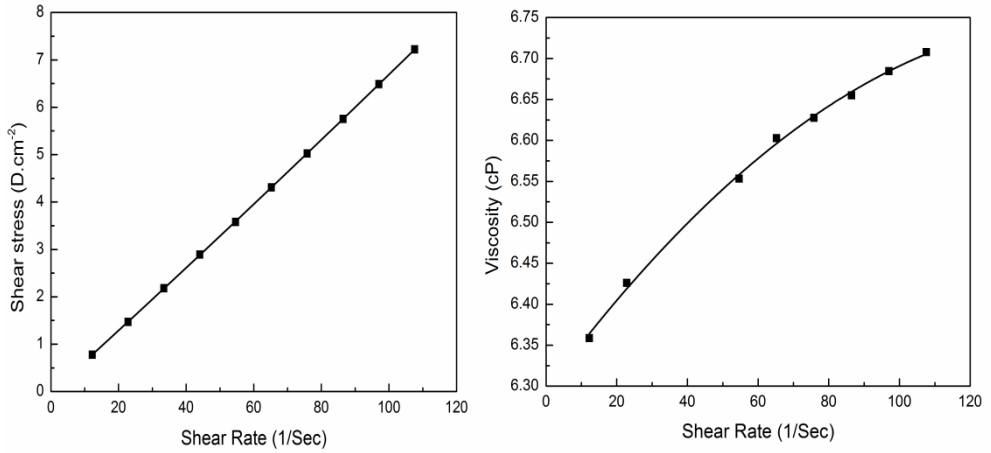
Shear stress (D.cm-2)
Shear Rate (1/Sec)
Viscosity (cP)
Shear Rate (1/Sec)

(g)

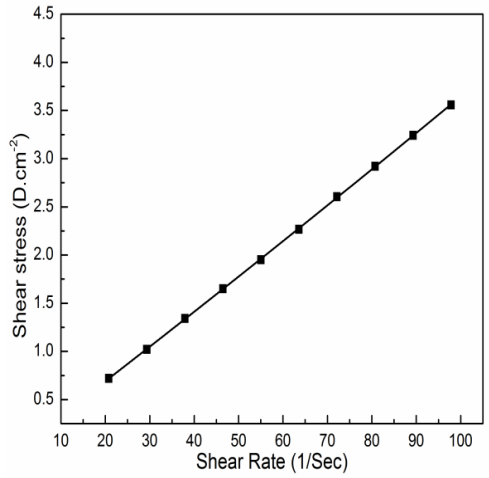

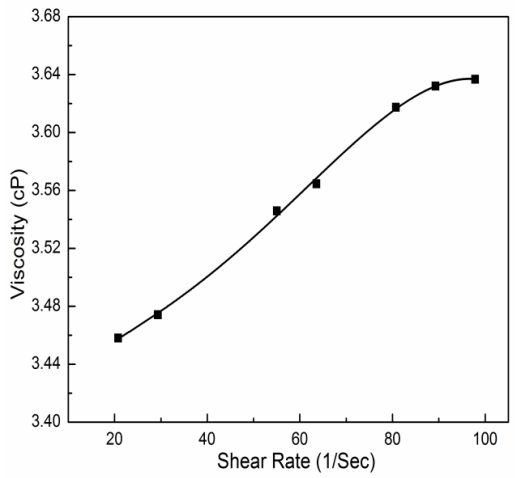

(h)

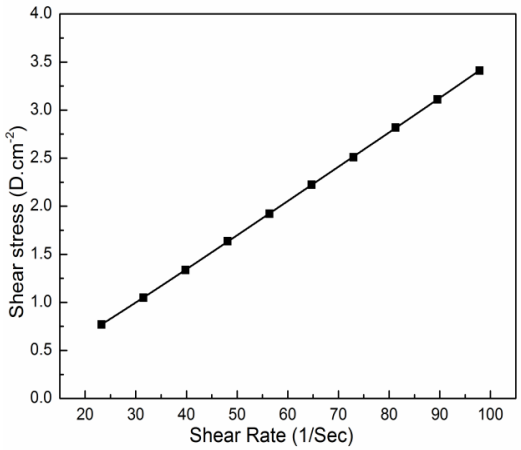

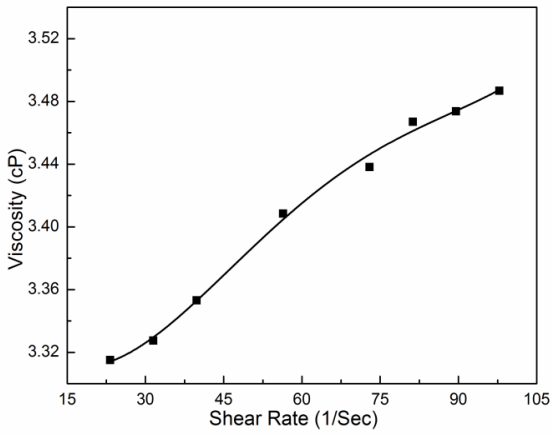

(i)

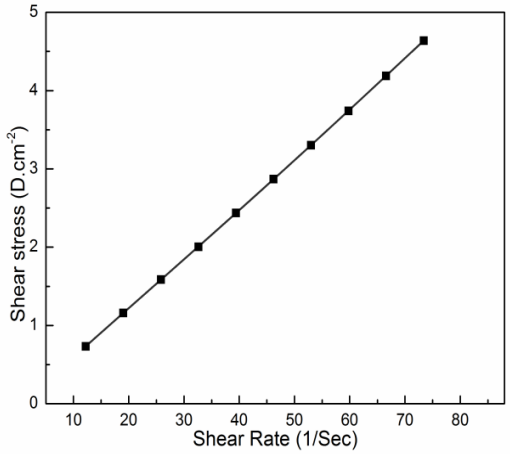

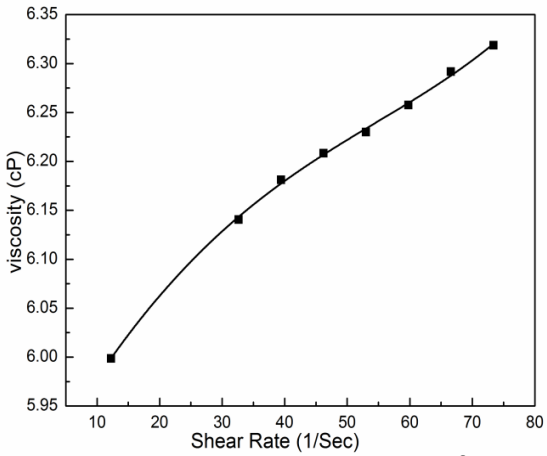

Figure (4.2): The apparent viscosities and shear stresses versus shear rates of (a) PHB, (b) PVAc and blends of PHB/PVAc of (c) 95/5, (d)90/10, (e) 85/15, (f) 80/20 (g) (75/25, (h) (70/30), (i) (65/35) thin films.

4.2 Fourier Transform Infrared Spectroscopy Analysis

Spectroscopic infrared techniques were used to verify PVAc blending to the PHB sample. The IR spectroscopy analysis gives further insights into the chemical structure of the polymer and reflects the monomeric. **Figure 4.3.a** shows the FTIR spectra of the pure PHB thin film. The PHB shows strong bands intense ester carbonyl stretch at 1734 cm^{-1} (Nichols *et al.,* 1985) and a number of strong bands at wavenumber between 1453 cm^{-1} and 1058 cm^{-1} due to methyl (CH_3) and methylene (CH_2) deformations and C-O stretches at 1058-1101 cm^{-1}. At 1458 cm^{-1} there an asymmetric deformation band of CH_3 and CH_2 (Kansiz *et al.,* 2000; Lim *et al.,* 2003). The blend also shows sharp and small absorption at wavenumber 3436 cm^{-1}, 2976-2874 cm^{-1}, 1734 cm^{-1} and 1229 cm^{-1}, representing the presence of O-H carboxylic acid or ester, two bands of C-H stretching, strong absorption band of polyesters and absorption from the PHB carbonyl group due to the presence of C ═O band which is the C-O-C groups appear in the spectral region from 1058 cm^{-1} to 1379 cm^{-1} and at wavenumber 1300-1500 cm^{-1} is due to the presence of CH_2, CH_3. The blends gave a sharp and small absorption at 1058-1102 cm^{-1} C-O-C corresponding to sharp and small absorption broad around 614-1101 cm^{-1} of C-H and 1734 cm^{-1} is the carbonyl absorption of PHB in amorphous region and this shift also indicates that the hydrogen bonding interaction mainly exists in the amorphous region. The enhancement of the 1022 cm^{-1} band represents the symmetrical stretching of the ═C ―O ―C of PVAc (Nicho & Hu, 2000). FTIR spectra run on the same samples did not reveal any significant differences in the bands in this region because PVAc and PHB have same functional groups and also at lower wavenumber region, two principal bands for CH_3 bending in the PHB at peaks 826 cm^{-1} and 838 cm^{-1} are observed. These results are in agreement with

data from previous studies (Chiellini & Solaro, 2003; Lim *et al.*, 2003; Zaikov, 2005; Mousavioun *et al.*, 2012).

Figure 4.3.b shows the **FT-IR** spectra of pure PVAc thin film. The large vibration bands observed at 3630 cm^{-1}-3456 cm^{-1} are ascribed to the stretching O–H and moisture. The bands observed at 2960 cm^{-1}, 2926 cm^{-1}, 2851 cm^{-1} and 1378 cm^{-1} are ascribed to CH_3 asymmetric stretching, symmetric stretching and symmetric bending vibrations of pure PVAc, respectively. Obviously, the band at 1738 cm^{-1} is due to C=O and C-O stretching from acetate group from the PVAc. As can be seen, the band at 1432 cm^{-1} and 947cm^{-1} are ascribed to the CH_2 scissor and C-H bending vibrations of pure PVAc, respectively. Apparently, the band at 1255 cm^{-1} and 1036 cm^{-1} are ascribed to C–O–C symmetrical stretching and C–C stretches vibrations of pure PVAc, respectively The result obtained by this is exactly similar to that of other researchers (Selvasekarapandian *et al.*, 2005; Mansur *et al.*, 2008; Shah, 2012; Pal & Gautam, 2013).

Figure 4.3.c shows the **FTIR** of the PHB/PVAc (95/5) thin film blend. PHB/PVAc (95/5) blend gives a long and broad absorption at wavenumber 1734 cm^{-1} which is due to the C═O carbonyl group associated to PHB ester peak and a few acetate groups present in the blending. As can be seen, the increase in the PVAc concentration in the blended film causes a decrease in the intensity of the band C═O at 1734 cm^{-1} of the PHB. The O-H blends carboxylic gives a large and sharp absorption band at wavenumber 3435 cm^{-1}; bands of C-H asymmetric and symmetric stretching, strong, long and sharp absorption band of polyester at wavenumber 2975 cm^{-1}, 2934 cm^{-1}, 2874 cm^{-1} and a presence of C-H small bending peak at 1452 cm^{-1} (Zuber *et al.*, 2012). The peak at wavenumber 1379 cm^{-1} shows the presence of CH_3 small bending. Band stretching of the C-O-C groups appears in the spectral region from 1282 cm^{-1}. A small and sharp absorption peak at 1059 cm^{-1} -

980 cm^{-1} is due to CO banding. The band of C-H gives a small and sharp absorption broad between 624 cm^{-1}–980 cm^{-1} while the 1734 cm^{-1} is the carbonyl absorption of PHB (Xu *et al.*, 2006).

Figure 4.3.d–4.3.i shows the **FTIR** of the PHB/PVAc blends of 90/10, 85/15, 80/20, 75/25, 70/30 and 65/35. All ratios give a sharp absorption due to the C═O carbonyl group at wavenumbers of 1731.5, 1724, 1715, 1730, 1737.8 and 1729.5 cm^{-1} of the PHB ester peak. The increase in the PVAc concentration in the blend films causes a decrease in the intensity of the band C═O of the PHB. Also, the blends give a sharp and small absorption band at wavenumber 3435- 3192 cm^{-1} due to the O-H carboxylic acid and two bands of C-H stretching show strong, small and sharp absorption band of polyester at wavenumber 2932 cm^{-1}- 2874 cm^{-1} and also at 2724 cm^{-1}, with CH_2 scissor at 1454 cm^{-1}. The blends give a sharp and small absorption broad between 624.63 cm^{-1}- 975.69 cm^{-1} of C-H as the 1731.83 cm^{-1} is the carbonyl absorption of PHB in the amorphous region (Selvasekarapandian *et al.*, 2006; Xu *et al.*, 2006). All the data are summarized in **Table (4.1).**

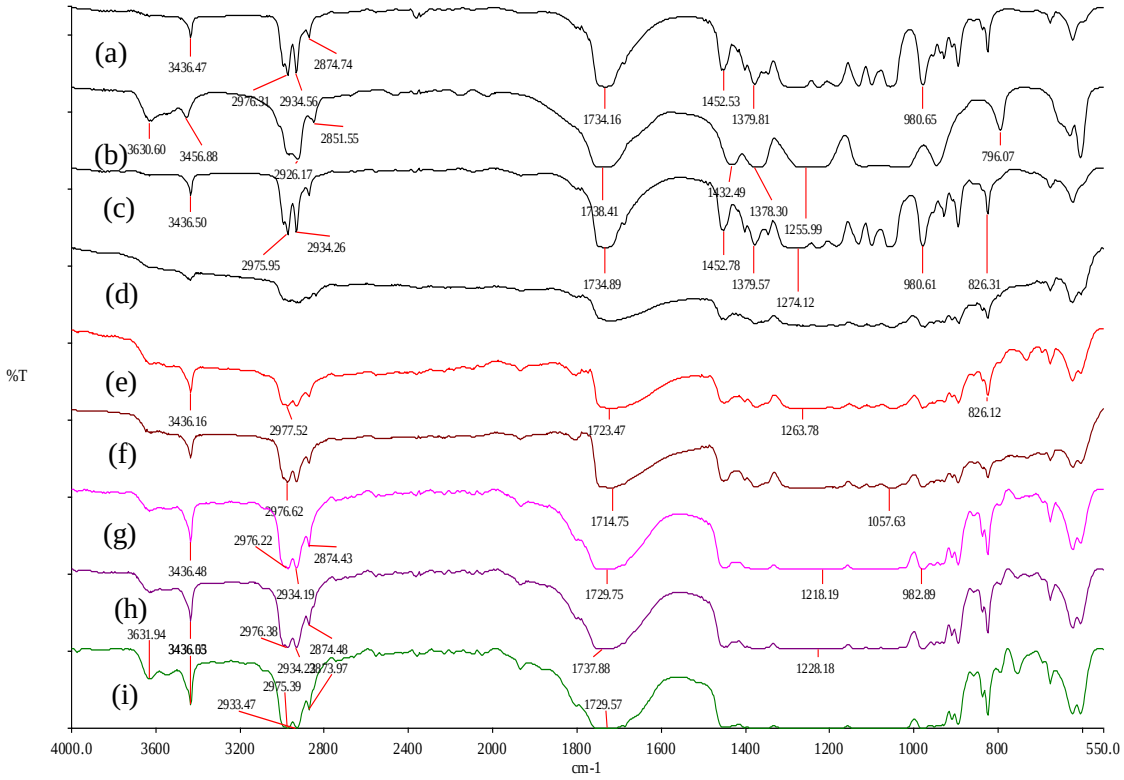

Figure (4.3): FTIR spectra of (a) pure PHB, (b) pure PVAc, and their blends of PHB/PVAc of (c) 95/5, (d) 90/10, (e) 85/15, (f) 80/20, (g) 75/25, (i) 65/35 thin films.

Table 4.1 FTIR characteristic bands of pure PHB and pure PVAc and PHB/PVAc blend films.

PHB/PVAc%	O-H	C=O	C-H $_{st}$	C-O-C	C-O
PHB	3436	1734	2976-2874	1276-980	1058-1101
PVAc	3456	1738	2960-2851	1255-980	1036-1102
PHB/PVAc(95/05)	3436	1734	2975 - 2934	1275 - 1380	1058-1102
PHB/PVAc(90/10)	3435.7	1731.5	2975 - 2875	1275 - 976	1048-1129
PHB/PVAc(85/15)	3436	1724	2977-2876	1263-979	1048-1127
PHB/PVAc(80/20)	3436	1715	2976-2875	1275-972	1058-1127
PHB/PVAc(75/25)	3436	1730	2976-2874	1275-983	1058-1101
PHB/PVAc(70/30)	3435	1737.8	2976-2874	1275-977	1058-1101
PHB/PVAc(65/35)	3436	1729.5	2975-2875	1276-975	1058-1127

4.3 Field Emission Scanning Electron Microscopy (FESEM) Measurements

The morphology of surface PHB/PVAc blends was investigated by field emission scanning electron microscopy (**FESEM**) and micrographs are shown in **Figure (4.4.a)**. As can be seen, pure PHB film shows smooth and homogeneous surface with some pores. The PHB phase appears in the micrograph as empty spaces. These micrographs show a clear difference in the morphology of the PHB and its composite (Abdelwahab *et al.*, 2012). The PHB/PVAc surface image was observed at voltage of 10 kV to examine the phase morphology. **Figure 4.4.b** shows surface of pure PVAc thin film that it has rougher surface. This result is in agreement with data from previous studies which showed that the pure PHB surface was smooth even though it is quite brittle (Xu *et al.*, 2006; Jelinska *et al.*, 2010; Srilalitha *et al.*, 2011).

(a) (b)

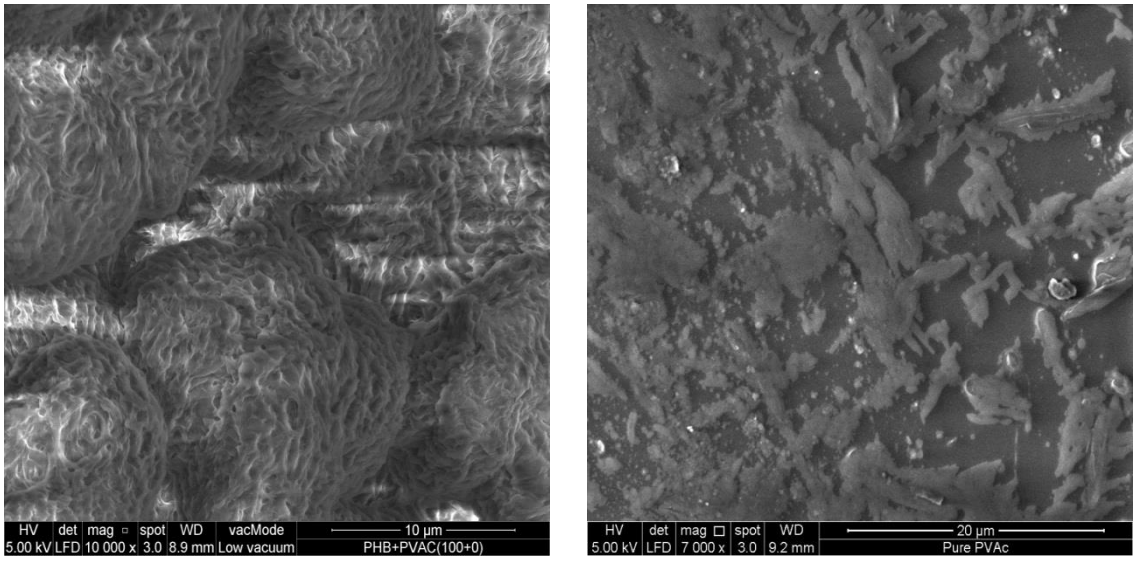

Figure (4.4): The scanning electron micrographs of (a) pure PHB and (b) pure PVAc thin films.

Figure 4.5 shows images of the top surface of PHB/PVAc blended films at different proportions. As can be seen, PHB/PVAc 95/5 shows smooth and homogeneous surface with small straps on the top of the surface while that of PHB/PVAc 90/10 no straps were seen. The surface of the blends PHB/PVAc 85/15 and 80/20 are homogeneous and have no interface layer. However, the blended films of PHB/PVAc show small pores in 90/10 and 80/20, which indicates that the PHB/PVAc 90/10 and 80/20 blends are immiscible in all the compositions. Observation from the PHB/PVAc blended films 75/25, 70/30 and 65/35 show smooth and homogeneous surface. The formation of homogeneous PHB and PVAc may be explained by interactions of hydrogen bonds between the functional groups of the blended components. Generally all the blended films display clear and homogeneous surfaces with almost no pores nor interface layer. These results are in agreement with data from previous studies (Zhang *et al.*, 1997; Xu *et al.*, 2006; Pachekoski *et al.*, 2009).

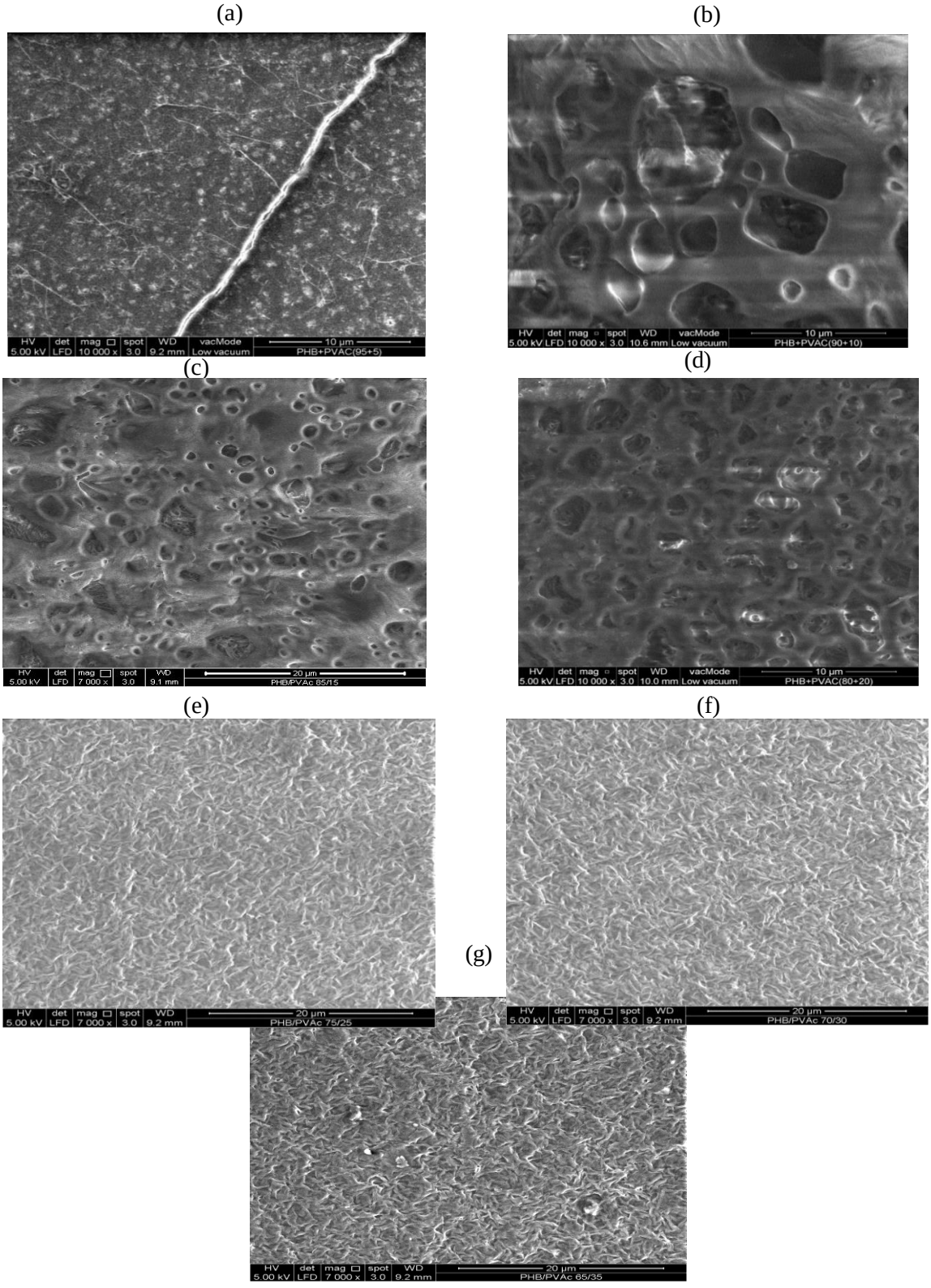

Figure 4.5: The scanning electron micrographs of PHB/PVAc blend thin films with various proportions (a) 95/5, (b) 90/10, (c) 85/15, (d) 80/20, (e) 75/25, (f) 70/30, (g) 65/35.

4.4 Thermal analysis

4.4.1 Thermogravimetric Measurements (TGA)

Polymers have different thermal stabilities depending on polymer structure and composition. TGA is advantageous in that it provides a rapid method to differentiate various polymers on the basis of temperature range, extent, rate, and activation energy of decomposition. The result shows that the addition of PVAc reduces the amount of material lost over the wide range of temperatures investigated (**Figure 4.6**). The lower weight loss is an indication that blends are thermally more stable than pure PHB. **Figure 4.6.a** shows the results of the thermogravimetric analysis of pure PHB thin film. There is no weight loss until 700 °C for all polymers. As can be understood, the pure PHB thin film displays a one–step degradation pattern. It began between 238.85 ℃ to 311.79 ℃ maximum degradation at (276.19 °C) with a weight loss of 97.569 %, which is attributed to the decomposition of the pure PHB (Ramachander *et al.*, 2002; Abdelwahab *et al.*, 2012). The recovered polymer rapidly degraded between 250 ℃ and 340 ℃ with a peak at 295 °C. The total weight loss of the sample at about 400°C is 97.569%. The remaining residue of the films which equals 2.431% is mostly due to the formation of organic complex. Similar behavior of the PHB thin film was reported in the literature. The degradation of PHB/PVAc blends by TGA have previously been reported by many researches (Shawaphun *et al.*; Lee *et al.*, 2002; Sombatmankhong *et al.*, 2006; Wang *et al.*, 2008; Zhu *et al.*, 2010; Zhang, 2011). They showed that the addition of PVAc lowers the onset of PHB degradation temperature. Although the addition of PVAc reduces the amount of material lost over a wide range of temperatures (Díez-Pascual & Díez-Vicente, 2014). **Figure (4.6.b)** shows the **TGA** curve of the pure PVAc film. The curve observed two weight loss transitions. Apparently, the pure PVAc thin film exhibited degradation

behavior intermediate to those of the pure PHB, exhibiting two degradation peaks at 366.55 ℃ and 454.37 ℃, respectively. The two–step thermal degradation which began between 280.52 ℃ to 404.34 ℃ with weight loss of 67.413 %, is attributed to the decomposition of pure PVAc. The second step began around 423.24 ℃ to 535.72 ℃ and weight loss of 19.875%. The remaining residue of the films which was 12.712 % is mostly due to the formation of organic compounds. The total weight loss of the sample was at about less than 900 ℃. Similar behaviour of PVAc film was reported in the literature (Chakraborty *et al.*, 1999; Sivalingam *et al.*, 2004; Sivalingam & Madras, 2004; Wu *et al.*, 2009; Wei & Huang, 2010). The thermal data are summarized in **Table 4.2.**

As can be seen **Figure (4.6.c)**, the thin film of PHB/PVAc exhibits a one–step degradation pattern. It begins from 237.67 ℃ to 308.33 ℃ with peak (290 ℃) and a weight loss of 95.623 % **Figure (4.7.d)** shows three weight loss transitions of PHB/PVAc (90/10) with an initial weight loss of 82.415% in the temperature range of 254.57 ℃ to 315.14 ℃, the second step begins around 316.58 ℃ to 377.87 ℃ with peak (355.53 ℃) and a weight loss of 6.126% while the third step begins around 434.11 ℃ to 501.89 ℃ with peak 484.51 ℃ and a weight loss of 7.442%. The **TGA** of PHB/PVAc (85/15) thin film shows three weight loss transitions (**Figure 4.6.e).** The film exhibits a three–step degradation pattern. It shows an initial weight loss of 85.432 % in the temperature range of 264.95 ℃ to 313.22 ℃ with peak 279.79 ℃. The second step begins around 313.22 ℃ to 396.23 ℃ at peak 360.23 ℃ with a weight loss of 8.753 %. The third step begins around 425.52 ℃ to 502.25 ℃ with peak at 474.86 ℃ and a weight loss of 2.169 %. **Figure 4.6.f** shows two weight loss transitions are observed in the TGA curve of PHB/PVAc (80/20). The film exhibits a two–step degradation pattern. The curve shows an initial weight loss of 83.891% in the temperature range of 254.83 ℃ to 312.98

°C. The second step begins around 313.90 °C to 380.36 °C with peak 353.67 °C and a weight loss of 10.135 %. The third step begins around 434.82 °C to 480.97 °C with peak 463.11 °C and a weight loss of 3.137 %. **Figure 4.6.g** shows three weight loss transitions for the 75/25 blend. The film exhibits a three–step degradation pattern. It begins from 248.83°C to 312.96 °C with peak at 278.45 °C and a weight loss of 80.614%. The second step began around 311.50 °C to 386.55 °C at peak 360.59 °C and a weight loss of 12.155%. The third step begins around 432.46 °C to 495.86 °C at peak 471.69 °C with a weight loss of 2.804%. **Figure 4.6.h** shows three weight loss transitions for the 70/30 blend film. The three–step degradation pattern begins from 239.38 °C to 315.82 °C with peak at 274.14 °C and a weight loss of 78.656 %. The second step begins from 315.82 °C to 383.69 °C with weight loss 12.956 %. The third step begins around 382.98 °C to 490.14 °C with weight loss of 3.586 %. **Figure 4.6.i** shows three weight loss transitions in the ratio (65/35). As can be seen in **Table 4.2**, the film exhibits a three step degradation pattern. The curve shows an initial loss of weight around 73.115% in the temperature range of 254.16 °C to 310.30 °C. The second stage began around 310.30 °C to 387.48 °C with peak at (358.15 °C) and weight loss 16.882%. The third step begins around 432.39 °C to 556.59 °C and a weight loss of 6.173 %.

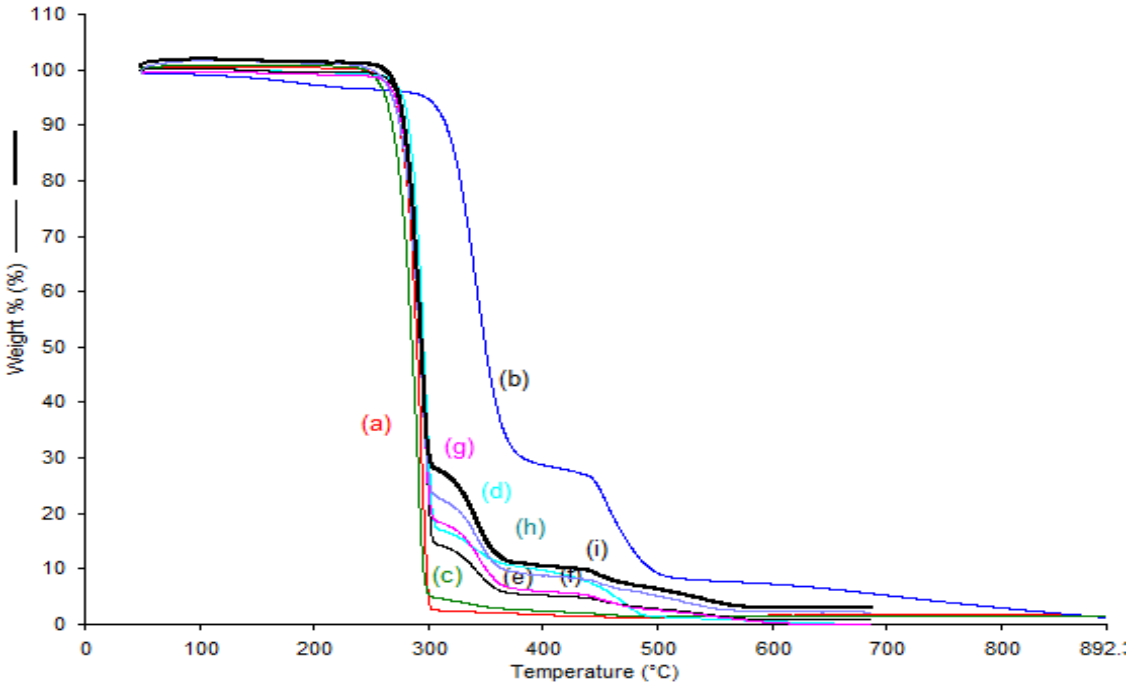

Figure (4.6): TGA curves of (a) pure PHB, (b) pure PVAc and blends of PHB/PVAc (c) 95/5, (d) 90/10, (e) 85/15, (f) 80/20, (g) 75/25, (h) 70/30, (i) 65/35.

Table 4.2 shows the weight loss (%) of the thin films of pure PHB, pure PVAc and their blends

Materials	First step	Second step	Third steps
	Weight% Temperature °C	Weight% Temperature °C	Weight% Temperature °C
Pure PHB	97.569% 238.85 to 311.79	**	**
Pure PVAc	67.413% 280.52 to 404.34	19.875% 423.24 to 535.72	**
PHB/PVAc 95/05	95.623% 237.67 to 308.33	**	**
PHB/PVAc 90/10	82.415% 254.57 to 315.14	6.126% 316.58 to 377.87	7.442% 434.11 to501.89
PHB/PVAc 85/15	85.432% 246.95 to 313.22	8.753% 313.22 to 396.23	2.169% 425.52 to 502.25
PHB/PVAc 80/20	83.891% 254.83 to 312.98	10.135% 313.90 to 380.36	3.137% 432.82 to 482.25
PHB/PVAc 75/25	80.614 248.83 to 312.96	12.155% 311.50 to 386.55	2.804% 320.46 to 495.86
PHB/PVAc 70/30	78.656% 239.38 to 315.82	12.956% 315.82 to 383.69	3.586% 383.8to 490.14
PHB/PVAc 65/35	73.115% 254.16 to 310.30	16.882% 310.30 to 387.48	6.173% 432.39 to 556.59

** Not detected

From **Table 4.2,** it is clear that all the blend thin films are highly associated with the interactions between PHB and PVAc through hydrogen bonding formation between their functional groups (Xu *et al.*, 2006). PHB/PVAc (70/30) and PHB/PVAc (65/35) have a lower thermal stability than the other composition, where weight lost % are higher. The weight % of the second step was also decreased with increasing PVAc contents (Zulfiqar & Ahmad, 2001; Aoyagi *et al.*, 2002; Xu *et al.*, 2006).

4.4.2 Differential Scanning Calorimetry Measurements (DSC)

The **DSC** measurement is particularly useful in this study of crystallization because it enables direct measurement of thermodynamic properties, melting temperature and heat of fusion. The **DSC** thermograms of the blends are shown in **Figure (4.7).** The sample weight was between 3 mg to 10 mg of PHB and their blends. The value of T_m was taken as the melt peak temperature. The DSC curve of PHB film shows a long, sharp peak endothermic around 176 ℃ (**Figure (4.7. a**)) while PVAc film shows a long, sharp endothermic peak around 201.49 °C **Figure (4.7.b**) (Song & Long, 1991; Pal & Gautam, 2013). The pure PHB shows two endothermic peaks between 158 ℃ and 176 °C and the peak at 176 ℃ is attributed to the melting of the crystalline film, which means the existence of a main crystalline region with more perfect structure (Zhang *et al.*, 1997; Abd-El-Haleem *et al.*, 2007a). All compositions exhibited a broad endothermic peak at different position ranging from about 160-176.49℃. PHB/PVAc (95/5) shows a sharp endothermic peak around 172.91 °C **Figure (4.7.c)** while the PHB/PVAc (90/10) film shows a broad endothermic peak at around 174.41 ℃ **Figure (4.7.d)**. The PHB/PVAc (85/15) shows a broad endothermic peak around 174.03 ℃ **Figure (4.7.e)**, which PHB/PVAc (80/20) shows a broad endothermic peak at 172.92 ℃ **(Figure 4.7.f)**. PHB/PVAc (75/25) shows two endothermic peaks between 159.60 and 175.51 °C **Figure (4.7.g)** while PHB/PVAc (70/30) shows one endothermic peak at 175.21 ℃ (**Figure 4.7.h)**. PHB/PVAc (65/35) shows a sharp endothermic peak at around 175.07 °C **(Figure 4.7.i)**. The melting enthalpy (ΔH) was obtained from the area of the two endothermic peaks. The DSC data of the blends are summarized in **Table (4.3)**. The DSC curve of pure PHB film shows a sharp exothermic peak around 73.06 °C while PVAc film shows a small endothermic peak at 40.09 °C (Dias *et al.*, 2009). Also the DSC curve of the

second run for PHB/PVAc (95/5) shows a sharp endothermic peak at around 56.37 ℃. PHB/PVAc (90/10) appears on a broad endothermic peak around 64.36 ℃ while PHB/PVAc (85/15) appears on a broad endothermic peak at 72.91 ℃.

PHB/PVAc (80/20) appears on a broad endothermic peak around 75.55 ℃ while the PHB/PVAc (75/25) appears on a broad endothermic peak at 75.55 ℃. The PHB/PVAc (70/30) appears on a broad endothermic peak around 75.91 ℃ but PHB/PVAc (65/35) has no endothermic peak, which means no melting transition (Abd-El-Haleem *et al.*, 2007b; Wang *et al.*, 2008; Pachekoski *et al.*, 2009). The DSC data of the blends are summarized in **Table (4.3).** The crystallization behavior of the polymers was tested using **DSC**. (Song & Long, 1991; Pal & Gautam, 2013).

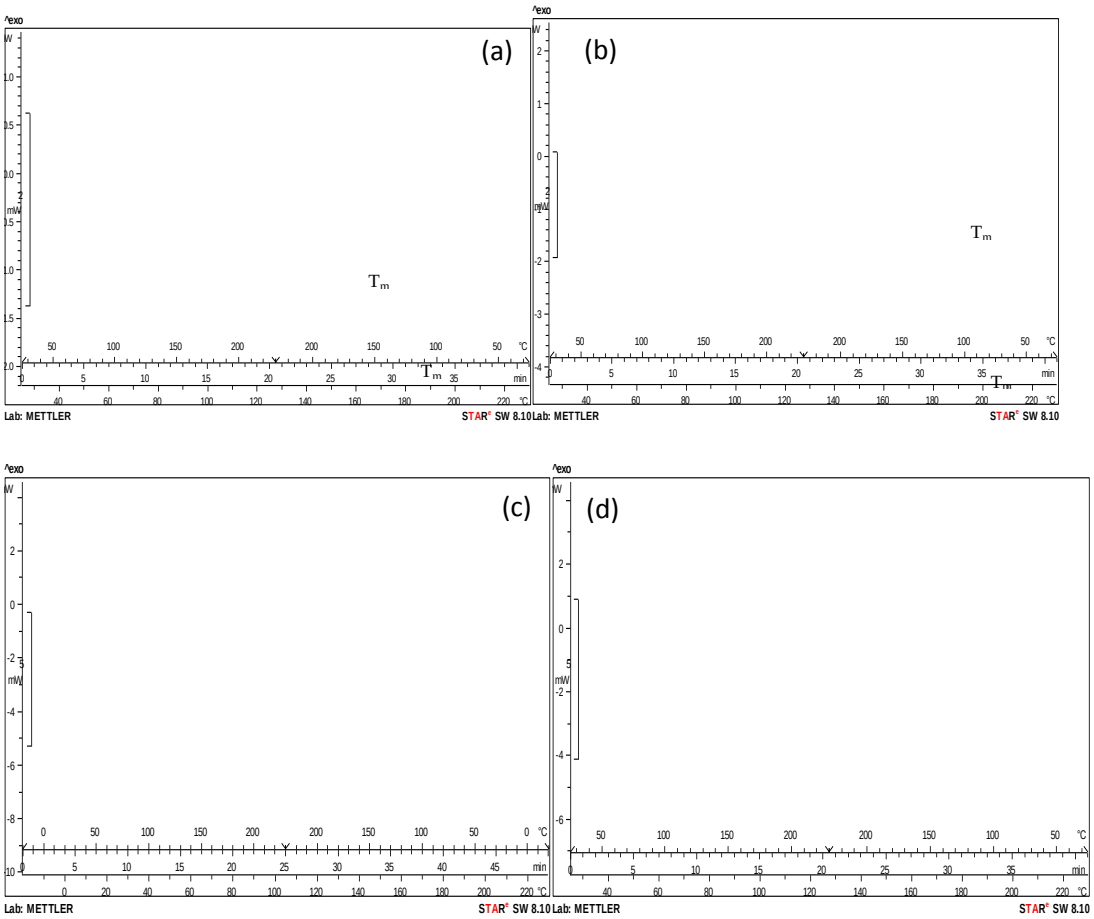

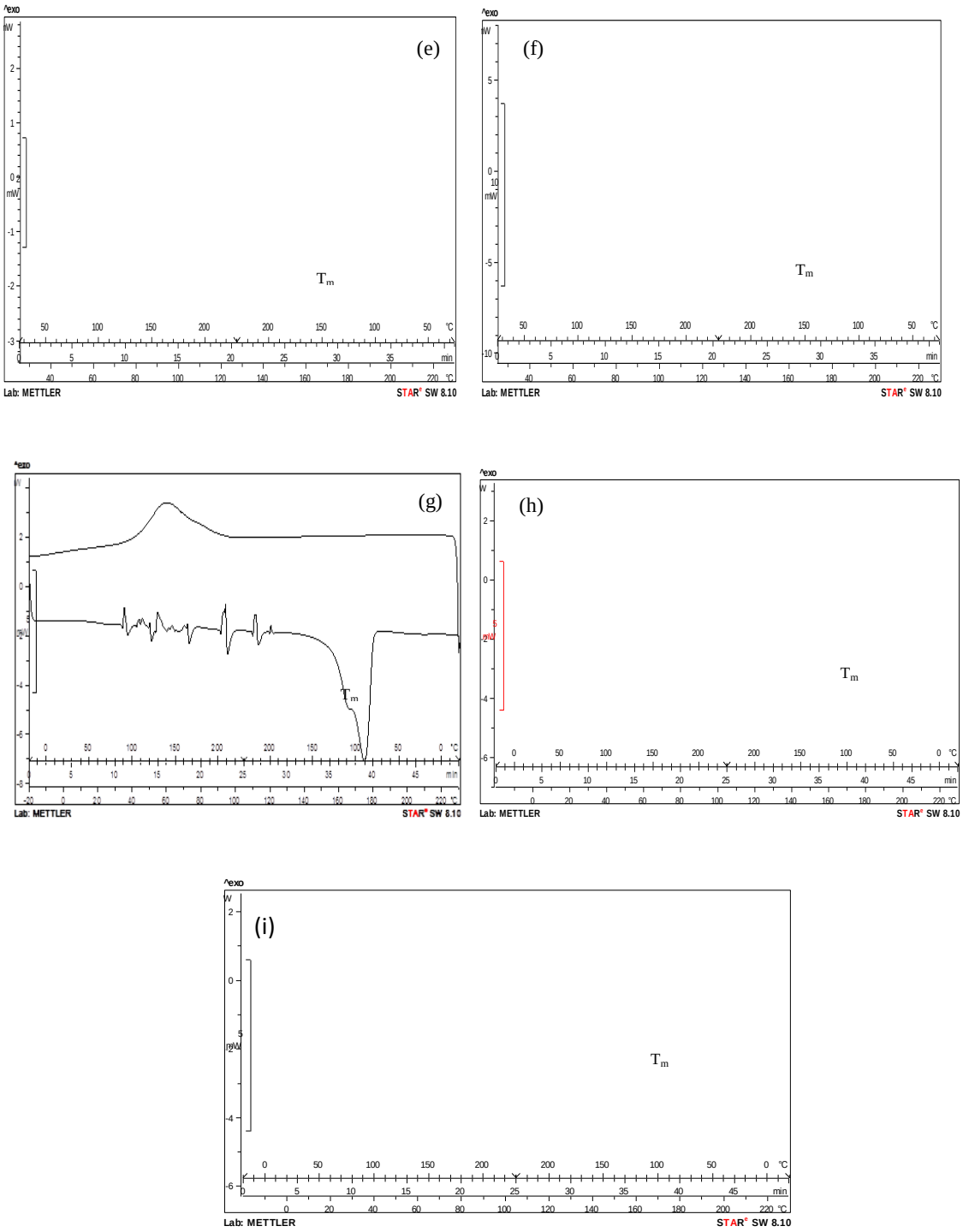

Figure 4.7: The DSC for two heating-cooling cycle curve of (a) pure PHB, (b) pure PVAc and blends of PHB/PVAc of (c) 95/5, (d) 90/10, (e) 85/15, (f) 80/20, (g) 75/25, (h) 70/30 and (i) 65/35

Table 4.3 Thermal properties of pure PHB and pure PVAc films together with their blended films with different PVAc contents (Zhang *et al.*, 1997).

Blend composition PHB/PVAc	**100/0**	**95/5**	**90/10**	**85/15**	**80/20**	**75/25**	**70/30**	**65/35**	**0/100**
T_m °C (first run)	176	172.91	174.41	174.03	172.92	175.21	175.21	175.07	201.49
T_c °C (second run)	73.06	56.37	64.36	72.91	75.55	75.55	73.91	**	40.09
ΔT °C	102.9	116.54	110.05	101.12	97.37	99.66	101.3	175.07	161.4
ΔH (J/g)	106.6	101.27	95.94	90.61	85.28	79.95	74.62	69.29	127

**** = not detected**

Calculated from the relation $\Delta T = T_m - T_c$.

$\Delta H_f = \Delta H_{f\ PHB} \times W_{PHB}$

The T_m, T_c and ΔH were taken from the peak values of the respective endothermic or exothermal processes in the DSC curves. As shown in **Table (4.3)**, PHB/PVAc (70/30), PHB/PVAc (75/25) and PHB/PVAc (65/35) have higher thermal stability than the others compositions, where the T_{ms} are higher. T_m in the first run heating of PHB/PVAc blends was slightly increased when PHB/PVAc increased; the T_m of the second heating run was also decreased. With increasing PVAc contents, melting points of the blends increase. This was clearly manifested in the first heating run and increased in other compositions. If blending results in a material having a lower T_g it means that the blend has more flexible chains thus lowering stiffness as well as improving processability. On the other hand, if the blend has a higher T_g and a higher melt viscosity, there would be an improvement in prcessability with no change in chain stiffness (Shawaphun *et al.*, 2011).

4.5 X-ray diffraction

The X-ray diffraction (XRD) patterns from pure PHB thin film and pure PVAc thin film are shown in **Figures (4.8)** and **(4.9)**. The interlayer distance was calculated from the angular position 2θ using the Bragg formula, $\lambda=2d\sin\theta$; (wavelength (λ) of the X-ray was 0.154 nm. Thin film X-ray difractograms were recorded in a diffraction angle (2θ) range of 5^0 - 80^0 using a step size of 0-03° under an exposure time of 96.4 s.

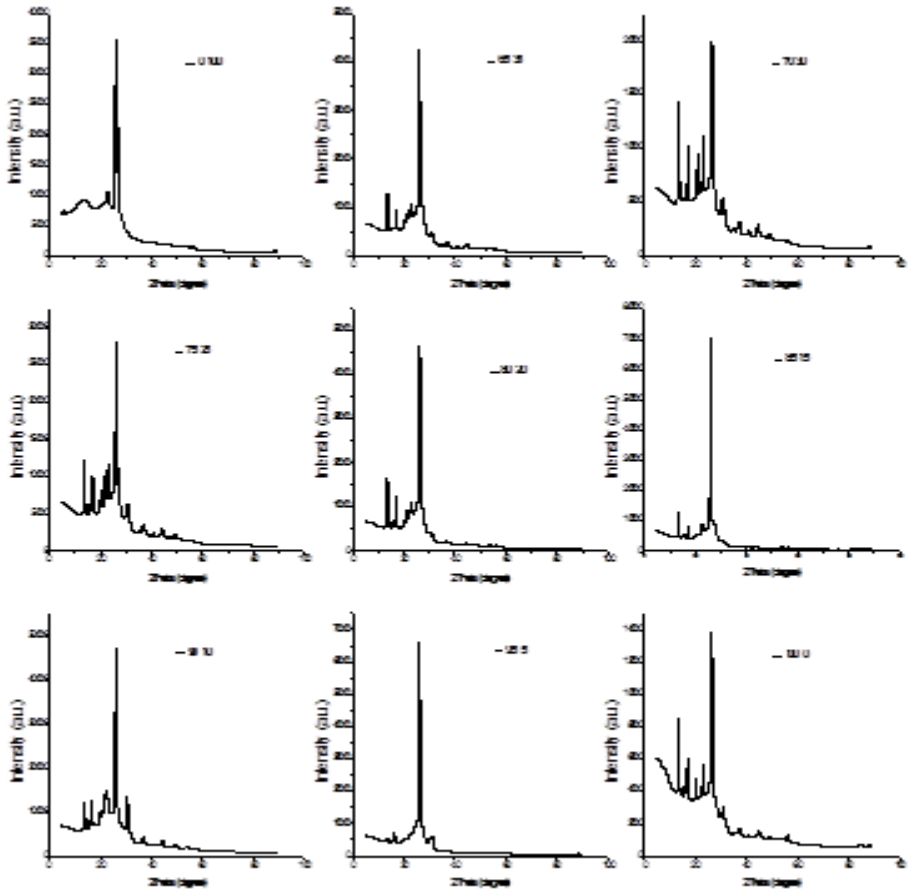

Figure (4.8): Typical XRD pattern for all proportions blends.

The XRD analysis is a useful tool in determining the structure and crystallization of polymer matrices. The XRD pattern of pure PHB is shown in **Figure 4.8.** The diffraction patterns of PHB/PVAc 95/05, 90/10, 85/15, 80/20, 75/25, 30/70 and 65/35 are shown in **Figure (4.9. a-i).**

Figure 4.9.a shows the XRD pattern of the pure PHB thin film. It shows high peak at $\theta = 26.07$ and the crystallinity calculated from High Score Plus is 73.58% (Abdelwahab *et al.*, 2012). The intensities of the main reflection peaks were found to decrease with increasing the PVAc contents (Saad & Seliger, 2004).

Figure 4.9.b shows the **XRD** pattern of pure PVAc thin film (Baskaran *et al.*, 2006). It shows the high peaks at $\theta = 26$ and the crystallinity calculated from High Score Plus is 52.46%. The XRD pattern of pure PVAc shows low crystallinity or amorphous nature (Baskaran *et al.*, 2006; Khan *et al.*, 2009). **Figure 4.9.c** shows the XRD pattern of the PHB/PVAc (95/5) blend film. It shows a high peak at θ=26.15 and the crystallinity calculated from High Score Plus is 60.92% (XRD program). The XRD patterns of blends of PHB/PVAc of the various compositions show that as the amount of the PHB in the blend increases, crystallinity increases. **Figure 4.9.d** shows a peak at $\theta = 26$ and the crystallinity calculated from High Score Plus is 51.34% in the PHB/PVAc (90/10) blend film. **Figure 4.9.e** shows the XRD pattern of PHB/PVAc 85/15 blend film. It shows a peak at $\theta = 26.01$ and the crystallinity calculated from High Score Plus is 53.69%. **Figure 4.9.f** shows the XRD of PHB/PVAc (80/20) blend film. It shows peak at $\theta = 26.25$ and the crystallinity calculated from High Score Plus is 52.98%. **Figure 4.9.g** shows the **XRD** result of PHB/PVAc (75/25) blend film. It shows a peak at $\theta = 26.6$ and the crystallinity calculated from High Score Plus is 51.30%. **Figure 4.9.h** shows the XRD of PHB/PVAc (70/30) blend film. It shows a peak at θ=26.2 and the crystallinity

calculated from High Score Plus is 49.98%. **Figure 4.9.i** shows the **XRD** pattern of PHB/PVAc (65/35) blend film. It shows the peak at θ= 26.2 and the crystallinity calculated from High Score Plus is 50 %. These results are in agreement with data from previous studies (Saad & Seliger, 2004; Sato *et al.*, 2006; Khan *et al.*, 2009; Nasar *et al.*, 2009). In addition, smaller peaks at different θ appeared in the XRD curves of PHB/PVAc blend films with various blend ratios from 95/5 to 65/35ranging from 13° - 22°. This is because increasing the PVAc content in the blend reduces the PHBcrystallinity. The XRD patterns of the blends of PHB/PVAc of the various compositions show that as the amount of the PHB in the blend decreases, crystallinity decreases and reaches a high intensity in the composition PHB/PVAc (70/30). This 70/30 exhibits three intense peaks at 2θ values of 13.54°, 16.55° and 22.57°. These peaks are assigned to increase the PVAc content. **Table 4.4** are summarized all data.

Table 4. 4 : The XRD data of pure polymers and their blends.

	2θ	**Crystallinity**
PHB	13.3°,17°,21.2°, 26.07°	73.58%
PVAc	12.7°, 26°	52.46%
PHB/PVAc (95/5)	13.7°,16.9°,21°, 26.15°	60.92%
PHB/PVAc (90/10)	13.05°,17.1°,21.9°, 26°	51.34%
PHB/PVAc (85/15)	13.3°, 17.1°, 22.1°, 26.01°	53.69%
PHB/PVAc (80/20)	13.6°,17.2°, 21.9°, 26.25°	52.30%
PHB/PVAc (75/25)	13.78°,17.2°,22.1°, 26.6°,	51.30%
PHB/PVAc (70/30)	13.6°,16.9°, 22°, 26.2°	50%
PHB/PVAc (65/35)	13.8°, 17.04°, 21.11°, 26.2°	49.98%

From Table 4.4, as the PVAc content increase from 5 ml – 35 ml and may have interfered with crystallization of PHB, it is clear that all blend thin films show decrease in crystallinity from 73.58% to 49.98%. The presence of amorphous PVAc significantly reduces the crystallinity of the PHB/PVAc samples.

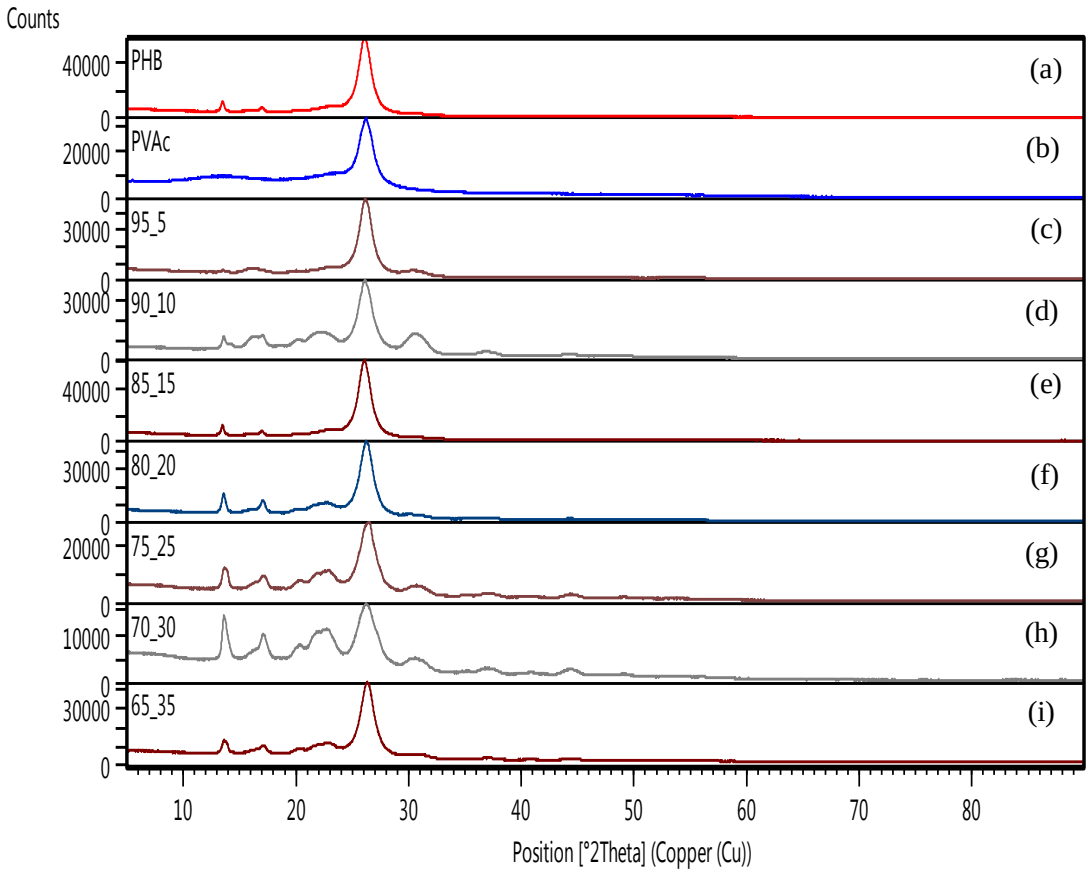

Figure (4.9): Typical XRD pattern of (a) pure PHB, (b) pure PVAc and blends of PHB/PVAc (c) 95/5, (d) 90/10, (e) 85/15, (f) 80/20, (g) 75/25, (h) 70/30, (i) 65/35 thin films.

4.6 BIODEGRADATION

Biodegradation plastics is an attractive route to environmental waste management and can replace conventional polymers when recovery for recycling or incineration is difficult and/or not cost-effective. Research has focused on both the addition of biodegradable polymers to common thermoplastics and on purely biodegradable, natural and synthetic polymers. Among these, poly(3-hydroxybutyric acid) (PHB), has been developed and investigated as one of the potential candidates for biodegradable plastics to reduce pollution caused by synthetic polymer waste. PHB, saturated linear polyester behaving like a conventional thermoplastic material, is a polymer of poly(3-hydroxybutyric acid) produced via biosynthesis by a wide variety of bacteria. PHB serves as an intracellular storage material for carbon and energy and is accumulated as granules within the cytoplasm of the bacteria (Verhoogt *et al.*, 1994; Park *et al.*, 2001). One of the unique properties of biological PHA materials is their biodegradability in various environments. The biodegradability of PHA in natural environments such as soil has been studied and characterized by TGA and FTIR.

4.6.1 Fourier Transform Infrared Spectroscopy (FTIR)

Figures 4.10 - 4.11 show the typical **FTIR** spectra of pure polymers and their blends thin films of the first week and fifth week. The small vibration band of CO appears at wavenumber 1735.8 cm^{-1} in the PHB and this band decreases in the blends which may be due to increase of PVAc. The O-H stretching band shows as broad peak at 3434 cm^{-1}. At wavenumber 1738 cm^{-1} the PVAc appears as sharp peak assign to C=O compared to their blends which show a broad peak with decreasing value. The spectra of the of CH_2, CH_3 asymmetric and symmetric stretchings appear at wavenumber region of 2900-2800 cm^{-1} in all samples (Bonartsev *et al.*, 2012). All buried blends contain some extra peaks compared to pure PHB and pure PVAc. IR spectra of PHB/PVAc show a strong

hydrogen bonded O-H stretching absorption around 3400 cm^{-1} and a prominent C-H stretching absorption around 2900-2800 cm^{-1}.

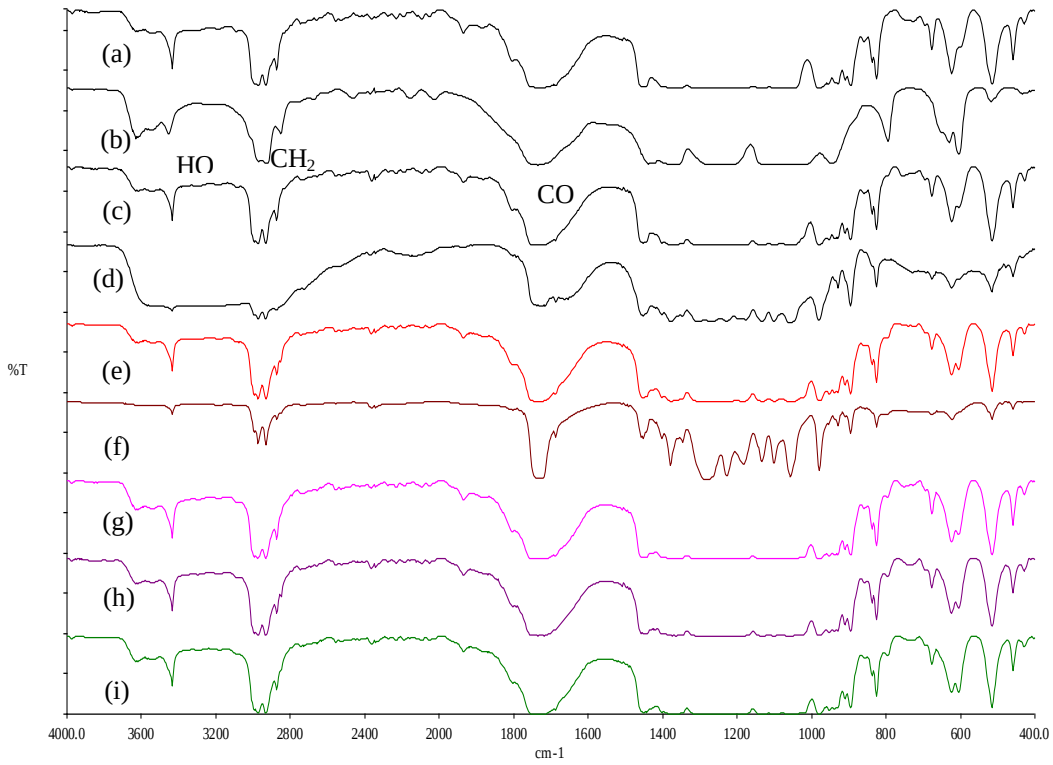

Figure 4.10: FTIR spectrum of (a) pure PHB, (b) pure PVAc and blends of PHB/PVAc of (c) 95/5, (d) 90/10, (e)85/15, (f) 80/20, (g) 75/25, (h)70/30, (i) 65/35 after the first week of degradation.

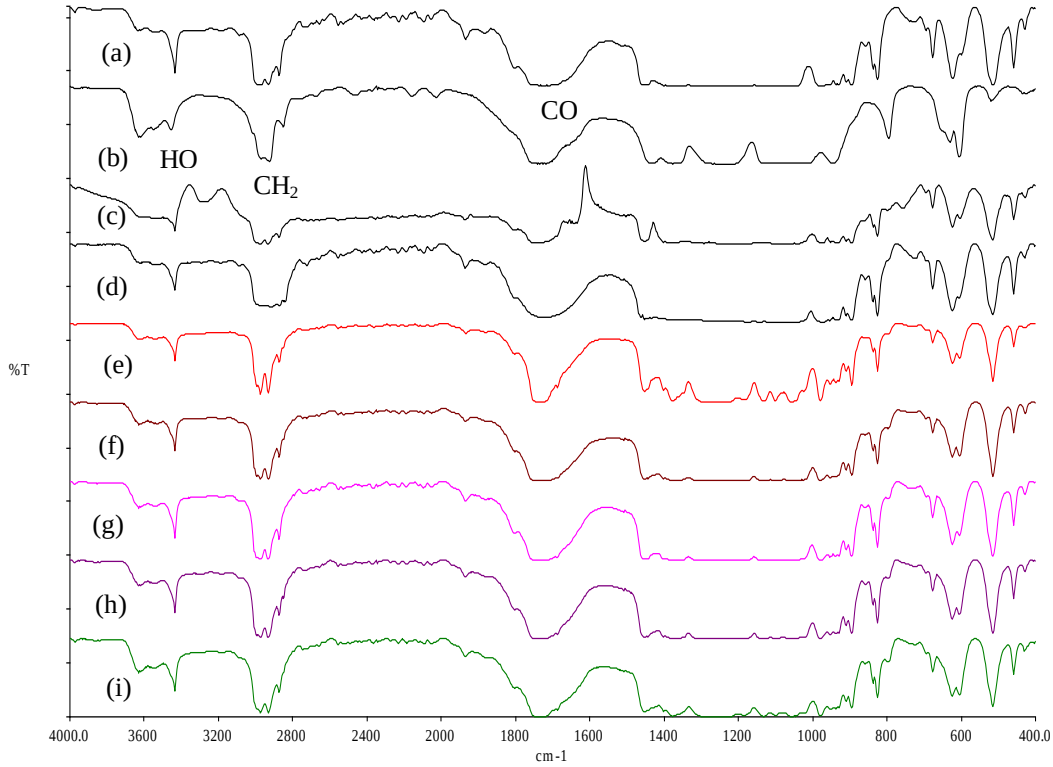

Figure 4.11: FTIR spectrum of (a) pure PHB, (b) pure PVAc and blends of PHB/PVAc of (c) 95/5, (d) 90/10, (e) 85/15, (f) 80/20, (g) 75/25, (h) 70/30, (i) 65/35 after the fifth week of degradation.

Table 4.5 (a-b) shows weight of all samples before and after degradation from first week to eighth week in the soil. The results show that the weights decrease significantly after degradation period. **Table 4.5.b** shows the data of seventh week and eighth week. In the eighth week the weight of the PHB/PVAc 65/35 raises from 0.0162 to 0.0166 g. **Table 4.5.a** displays all data on weight decrease in first and second week of degradation. The weight decreases after degradation in first week and second week. During the first week, PHB/PVAc 65/35 is 0.0142 g before degradation while after degradation is 0.0133 g. Comparing between different ratios of PHB/PVAc used, the weight of PHB/PVAc 95/05 ratio decreases from 0.0107 g to 0.0097 g in the first week and the weights continuously decrease during the eighth week but PHB/PVAc 65/35 degrades most compared to all other samples.

Table 4.5.a Weights of pure PHB and pure PVAc and their blends with different proportions before and after degradation from first week and second week.

Material	Weight before degradation (1-week)	Weight after degradation (1-week)	Weight before degradation (2-week)	Weight after degradation (2-week)
PHB	0.0107 g	0.0125 g	0.0062 g	0.0064 g
PVAc	0.0119 g	0.0025 g	0.0149 g	0.0152 g
PHB/PVAc 95/5	0.0107 g	0.0097 g	0.0100 g	0.0101 g
PHB/PVAc 90/10	0.0148 g	0.0150 g	0.018 g	0.0174 g
PHB/PVAc 85/15	0.0062 g	0.0069 g	0.0123 g	0.0124 g
PHB/PVAc 80/20	0.0120 g	0.0130 g	0.0165 g	0.0173 g
PHB/PVAc 75/25	0.0108 g	0.0110 g	0.0143 g	0.0157 g
PHB/PVAc 70/30	0.0126 g	0.0078 g	0.0070 g	0.0122 g
PHB/PVAc 65/35	0.0142 g	0.0133 g	0.0136 g	0.0143 g

Table 4.5.b Weights of pure PHB and pure PVAc and their blend with different proportions before and after degradation from seventh week and eighth week.

Material	Weight before degradation (7-week)	Weight after degradation (7-week)	Weight before degradation (8-week)	Weight after degradation (8-week)
PHB	0.0130 g	0.0134 g	0.0088 g	0.0083 g
PVAc	0.0131 g	0.0137 g	0.0224 g	0.0232 g
PHB/PVAc 95/5	0.0096 g	0.0097 g	0.0086 g	0.0089 g
PHB/PVAc 90/10	0.0157 g	0.0150 g	0.0158 g	0.0161 g
PHB/PVAc 85/15	0.0078 g	0.0072 g	0.0075 g	0.0081 g
PHB/PVAc 80/20	0.0118 g	0.0116 g	0.0149 g	0.0153 g
PHB/PVAc 75/25	0.0219 g	0.0140g	0.0148 g	0.0118 g
PHB/PVAc 70/30	0.0249 g	0.0250 g	0.0283 g	0.0282 g
PHB/PVAc 65/35	0.0207 g	0.0210 g	0.0162 g	0.0166 g

Table 4.6 (a-b) presents the FTIR spectral data of pure polymers and their PHB/PVAc blends at different proportions from first week to eighth week of degradation period. The CO wavenumber in pure PHB is 1734 cm^{-1} in the first week while it is 1719.40 cm^{-1} in the eighth week; the pure PVAc is 1736 cm^{-1} in the first week while it was 1728.37 cm^{-1} in the eighth week. Also the PHB/PVAc 95/05 shows the CO at 1728 cm^{-1} and 1718.9 cm^{-1} in the first week and eighth week respectively. However, the PHB/PVAc 85/25% shows the CO at 1726.3 cm^{-1} and 1719.9 cm^{-1} in the first week and eighth week respectively. The PHB/PVAc 70/30 shows the CO at 1735 cm^{-1} in the first week and 1719.8 cm^{-1} in the eighth week. For OH and CH peaks no significant different between the ratios are observed. From the FTIR data of the PHB/PVAc blends show slightly decreased in the CO values compared to pure polymers.

Table 4.6.a FTIR characterization of pure PHB and pure PVAc and PHB/PVAc blends films with different proportions after first week and second week of degradation.

	First week			**Second week**		
PHB/PVAc	O-H	C=O	C-H $_{st}$	**O-H**	**C=O**	**C-H $_{st}$**
PHB	3436-3630	1734,1689	2975-2875,1378	3436-3630	1731,1689	2976-2874,1379
PVAc	3457-3630	1736	2969-2851,1376	3457-3630	1732,1655	2974 - 2852,1377
PHB/PVAc 95/05	3436-3613	1728,1689	2976 – 2875,1398	3437-3635	1726,1689	2975 – 2874,1372
PHB/PVAc 90/10	3437-3621	1734,1688	2975 – 2874,1379	3436-3619	1728,1687	2934 – 2846,1343
PHB/PVAc 85/15	3437-3624	1726.3,16867	2976-2874,1378	3436-3624	1731,1688	2981-2874,1357
PHB/PVAc80/20	3436- 3613	1721,1687	2976-2874,1398	3436-3625	1732,1688	2975-2874,1399
PHB/PVAc 75/25	3437-3631	1732,1684	2977-2875,1368	3436-3630	1735,1688	2976-2875,1376
PHB/PVAc 70/30	3436-3631	1735,1686	2976-2874,1376	3436-3635	1730, 1689	2976-2874,1373
PHB/PVAc 65/35	3436-3631	1731,1687	2976-2874,1372	3436-3631	1732,1687	2975-2874,1373

Table 4.6.b FTIR characterization of pure PHB and pure PVAc and PHB/PVAc blend films with different proportions after seventh and eighth week degradation.

	Seventh week			**Eighth week**		
PHB/PVAc	**O-H**	**C=O**	**C-H $_{st}$**	**O-H**	**C=O**	**C-H $_{st}$**
PHB	3436	1719.3	2976-2874	3437	1719.40,1687	2977-2875,1379
PVAc	3456	1728.39	2960-2851	3452-3622	1728.37	2960-2850,1370
PHB/PVAc95/05	3437	1719	2976 - 2934	3437-3694	1718.95,1687	2977 – 2934,1358
PHB/PVAc 90/10	3436	1719	2932 - 2875	3435	1720,1687	2977 – 2874,1379
PHB/PVAc 85/15	3436	1719.2	2929-2876	3437	1719.95,1687	2977-2875,1387
PHB/PVAc 80/20	3436	1720	2976-2876	3437	1719.8,1687	2976-2876,1378
PHB/PVAc75/25	3435	1720	2976-2874	3437-3692	1719.65,1686	2977-2875,1378
PHB/PVAc 70/30	3435	1719	2976-2874	3437	1719.80,1687	2977-2874,1378
PHB/PVAc65/35	3436	1720	2975-2874	3439	1719.21,1687	2977-2875,1378

4.6.2 Thermogravimetric analysis (TGA)

The thermal data of the TGA of PHB/PVAc blends are summarized in **Table 4 .7. (a-b).** The first transition in the PHB is in the range 200 ℃ to 291 ℃ with loss weight 97.16%. The first transition in PVAc is from 278.9 ℃ to 387.9 ℃ with loss weight 69.11%. The second weight loss begins about 388 ℃ to 499 ℃ with weight 13.5%. The first stage is due to acetic acid at 280 ℃ and the second stage is due to the structural degradation of the polyene backbone occurs, leading to the aromatic and aliphatic hydrocarbon.

Figures 12 shows the results of TGA analysis of pure PHB and PVAc thin films from the first to the eighth week. PHB/PVAc blends have a different weight loss of around 80% - 73% with higher thermal stability than PHB. The results of TGA show that the addition of the PVAc caused improved the thermal stability of PHB component. From **Table 4.7** that the blend films of PHB/PVAc 65/35 and 80/20 have the lowest weight loss at temperature studied. This may be due to the increase in PVAc in the blending. This thermal stability behavior of the PHB/PVAc polymer blend was found to be similar with previous studies results (Mergaert *et al.*, 1993; Jendrossek *et al.*, 1995; Khanna & Srivastava, 2005). The degradation of PHB/PVAc blends occurs in more stages than PHB, suggesting blending PHB with PVAc has completely changed the decomposition of PHB.

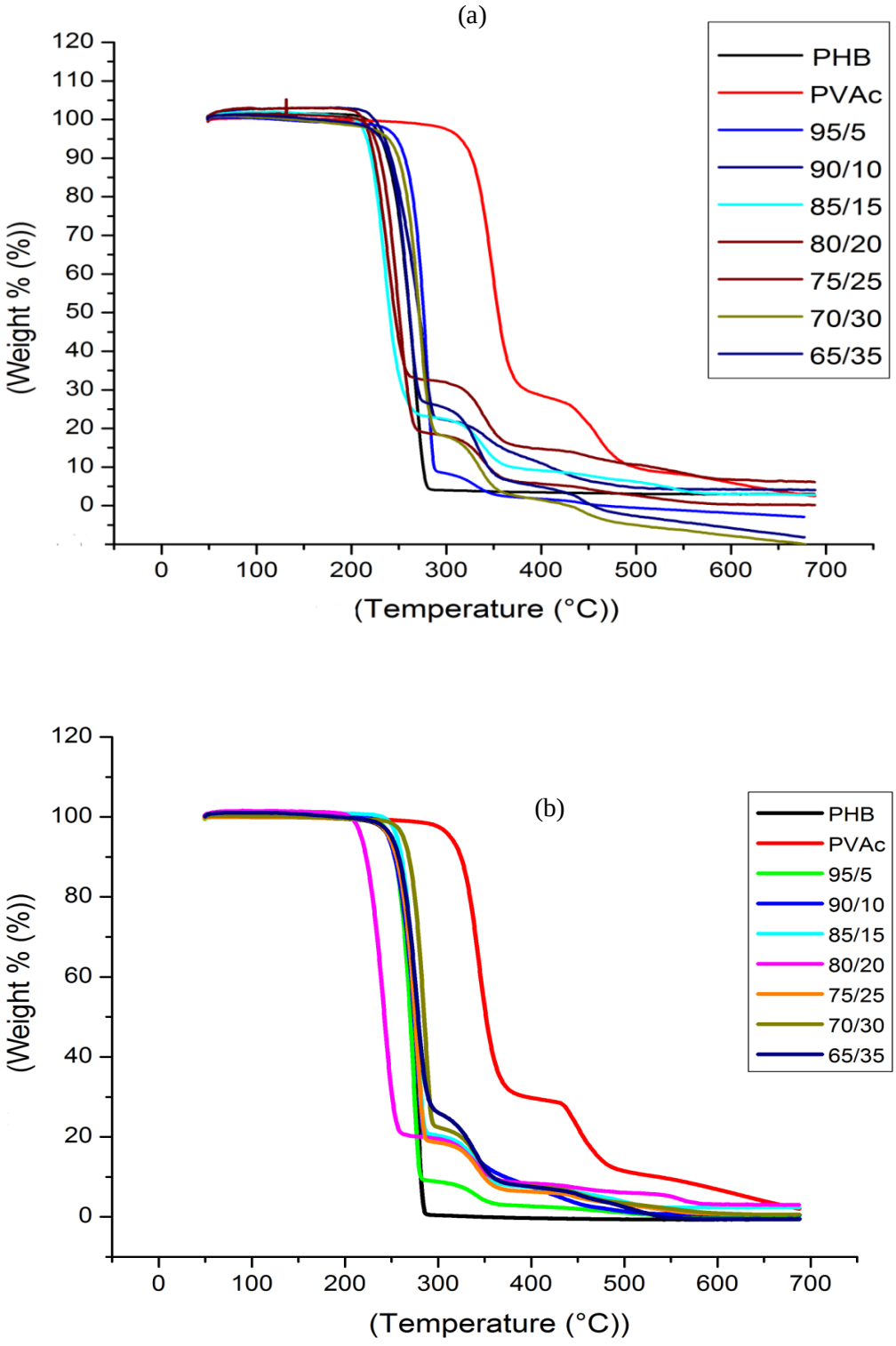

Figure 4. 12: TGA curves of pure PHB, pure PVAc and blends of PHB/PVAc after (a) the first week and (b) the eighth week of degradation.

Table 4.7.a TGA characterization of pure PHB and pure PVAc and their blend with different proportions after first week and second week of degradation in the soil.

Material	First week			Second week		
	First step	**Second step**	**Third step**	**First step**	**Second step**	**Third step**
	Weight% Temperature °C	Weight% Temperature °C	Weight% Temperature °C	Weight% Temperature °C	Weight% Temperature °C	Weight% Temperature °C
PHB	97.162 % 200.86 to 291.7	**	**	94.236 % 196.63 to 278	**	**
PVAc	69.114 % 278.9 to 387.9	13.151 % 388.6 to 449.9	**	66.826 % 292 to 394.7	17.757 % 413.8 to 501.5	**
PHB/PVAc 95/05	89.918 % 227.9 to 297.4	5.899 % 301.05 to 363.9	**	90.340 % 206.7 to 291.2	6.340 % 303.94 to 378.5	**
PHB/PVAc 90/10	80.620 % 199.4 to 299.6	9.210 % 303.12 to 379.17	5.718 % 393.4 to463.04	81.661 % 200.7 to 292.8	10.105 % 299.14 to 370.65	6.117 % 373.4 to478.27
PHB/PVAc 85/15	77.744 % 193.86 to 283	13.029 % 288.08 to 375.3	5.430 % 381.6 to 544.21	55.618 % 177.23 to 264	10.837 % 287.62 to 381.7	15.181 % 393.1 to 542.39
PHB/PVAc 80/20	70.282 % 193.3 to 285.1	17.438 % 291.37 to 391.53	5.017 % 432.86 to 542.1	72.942 % 186.3 to 281.6	18.851 % 282.34 to 382.57	5.716 % 382.57 to 472.2
PHB/PVAc 75/25	79.140 % 184.38 to 283.6	15.324 % 292.01 to 382.1	5.891 % 400.34 to 495.42	79.140 % 184.38 to 283.6	15.324 % 292.01 to 382.1	5.891 % 400.34 to 495.4
PHB/PVAc 70/30	82.877 % 208.26 to 301.9	16.878 % 301.9 to 380.59	7.591 % 388.4 to 493.35	65.724 % 223.47 to 297.4	12.978 % 302.23 to 385.8	5.075 % 381.7 to 470.69
PHB/PVAc 65/35	72.733 % 206.75 to 288.4	19.951 % 294.09 to 379.29	8.070 % 392.1 to 494.32	72.798 % 209.91 to 291.4	20.124 % 302.24 to 385.9	8.070 % 398.2 to 489.06

** Not detected

Table 4.7.b TGA characterization of pure PHB and pure PVAc and their blend with different proportions after seventh week and eighth week of degradation in the soil.

Material	Seventh week			Eighth week		
	First step	**Second step**	**Third step**	**First step**	**Second step**	**Third step**
	Weight% Temperature °C	Weight% Temperature °C	Weight% Temperature °C	Weight% Temperature °C	Weight% Temperature °C	Weight% Temperature °C
PHB	97.836 % 220 to 303.6	**	**	98.58 % 225.7 to 304.2	**	**
PVAc	66.826 % 287.7 to 397.6	17.070 % 405.6 to 504.5	**	68.84 % 284 to 401.1	19 % 408 to 522.7	**
PHB/PVAc 95/05	90.604 % 214.4 to 290.3	5.845 % 293.2 to 382.4	**	90.66 % 226.6 to 298	6.04 % 302.6to 400.4	**
PHB/PVAc 90/10	80.417 % 220.4 to 295.9	10.105 % 303.68 to 384.1	6.730 % 389.8 to 485.04	80.99 % 221.4 to 297.8	9.936 % 304.4 to 385.11	5.646 % 389.5 to 459.2
PHB/PVAc 85/15	78.360 % 226.25 to 293	12.816 % 302.35 to 380.5	2.812 % 394.9 to 484	80.15 % 226.9 to 299	12.35 % 304.9 to 380.24	3.68 % 399.8 to 500
PHB/PVAc 80/20	80.618 % 208.7to 289.4	12.135 % 295.85to 386.55	2.507 % 404.4 to 488.7	80.55 % 200 to 276.2	11.55 % 287.3 to 401	4.78 % 421.9 to 584.4
PHB/PVAc 75/25	79.893 % 228.2 to 302.7	12.480 % 307.07 to 382.4	3.330 % 390.29 to495.1	80.768 % 217.9 to 299.6	11.865 % 305.36 to 383.5	3.707 % 416.5 to 524.7
PHB/PVAc 70/30	77.190 % 235.2 to 309.2	13.223 % 314.11 to 378.2	4.690 % 385.2 to 503.56	76.835 % 238.9 to 301.5	13.727 % 306.44to 376.13	4.177 % 400.3 to 497.72
PHB/PVAc 65/35	72.844 % 217.2to 299.7	17.814 % 305.96 to 391.9	5.093 % 402.4 to 507.2	72.228 % 225.5 to 301.2	17.978 % 303.98 to 398.4	5.609 % 339.1 to 518.4

From the **Table 4.7 (a-d)**, PHB/PVAc 65/35 has a lower thermal stability than other compositions. Weight % in the first step of PHB/PVAc blends is slightly decreased when PVAc is increased in the blending; the weight % of the second step is also decreased, while increasing PVAc contents.

References

Abd-El-Haleem, D.A.M., AlMa'adeed, M.A., & Al-Thani, N. (2007). Physical and Chemical Properties of Polyhydroxyalkanotes Biodegradable Polymers Produced in Transgenic Yeasts. *Global Journal of Environmental Research,* **1** (2), 69-73.

Abdelwahab, M. A., Flynn, A., Chiou, B.-S., Imam, S., Orts, W., & Chiellini, E. (2012). Thermal, mechanical and morphological characterization of plasticized PLA–PHB blends. *Polymer Degradation and Stability*, **97** (9), 1822-1828.

Aoyagi, Y., Yamashita, K., & Doi, Y. (2002). Thermal degradation of poly[(R)-3-hydroxybutyrate], poly[ε-caprolactone], and poly[(S)-lactide]. *Polymer Degradation and Stability,* **76**(1), 53-59.

Baskaran, R., Selvasekarapandian, S., Kuwata, N., Kawamura, J., & Hattori, T. (2006). Conductivity and thermal studies of blend polymer electrolytes based on PVAc–PMMA. *Solid State Ionics,* **177** (26–32), 2679-2682.

Bonartsev, A., Boskhomdzhiev, A., Voinova, V., Makhina, T., Myshkina, V., Yakovlev, S., Zharkova, I., Filatova, E., Zernov, A., & Bagrov, D. (2012). Degradation of poly(3-hydroxybutyrate) and its derivatives: characterization and kinetic behavior. *Chemistry & chemical technology*, **6**(4), 385-392.

Chakraborty, M., Mukherjee, D. C., & Mandal, B. M. (1999). Interpenetrating polymer network composites of polypyrrole and poly(vinyl acetate). *Synthetic Metals,* **98** (3), 193-200.

Chiellini, E., & Solaro, R. (2003). *Biodegradable Polymers and Plastics*: Springer US.

Dias, D. S., Crespi, M. S., Kobelnik, M., & Ribeiro, C. A. (2009). Calorimetric and SEM studies of PHB–PET polymeric blends. *Journal of Thermal Analysis & Calorimetry*, **97** (2), 581-584.

Díez-Pascual, A. M., & Díez-Vicente, A. L. (2014). Poly(3-hydroxybutyrate)/ZnO bionanocomposites with improved mechanical, barrier and antibacterial properties. International journal of molecular sciences, 15(6),10950-10973.

EL-Hefian, E. A, Nasef, M. M., Yahaya, A. H., & Khan, R. A. (2010). Preparation and characterization of chitosan/agar blends: rheological and thermal studies. Journal of the Chilean Chemical Society, 55 , 130-136.

Jelinska, N., Kalnins, M., Tupureina, V., & Dzene, A. (2010). Poly (vinyl alcohol)/poly(vinyl acetate) blend films. Scientific Journal of Riga Technical University Material Science and Applied Chemistry, 1, 55-61.

Jendrossek, D., Frisse, A., Behrends, A., Andermann, M., Kratzin, H. D., Stanislawski, T., & Schlegel, H. G. (1995). Biochemical and molecular characterization of the Pseudomonas lemoignei polyhydroxyalkanoate depolymerase system. Journal of Bacteriology, 177(3), 596-607.

Guest, S., McGlone, F., Hopkinson, A., Schendel, Z. A., Blot, K., Essick, G. (2013). Perceptual and Sensory-Functional Consequences of Skin Care Products. Journal of Cosmetics, Dermatological Sciences and Applications, 3 (1A), 66-78.

Kansiz, M., Billman-Jacobe, H., & McNaughton, D. (2000). Quantitative determination of the biodegradable polymer poly(β-hydroxybutyrate) in a recombinant Escherichia coli strain by use of mid-infrared spectroscopy and multivariative statistics. Applied and environmental microbiology, 66 (8), 3415-3420.

Khan, M. S., Khalil, U., & Nasar, G. (2009). XRD Study of Binary Polymer Blend of PMMA/PVAC. J Pak Mater Soc, 3 (1), 22-26.

Khanna, S., & Srivastava, A. K. (2005). Recent advances in microbial polyhydroxyalkanoates. Process Biochemistry, 40(2), 607-619.

Lee, S. N, Lee, M. Y., & Park ,W. H. (2002). Thermal stabilization of poly(3-hydroxybutyrate) by poly(glycidyl methacrylate). Journal of Applied Polymer Science, 83 (13), 2945-2952.

Lim, S. T., Hyun, Y. H., Lee, C. H., & Choi, H. J. (2003). Preparation and characterization of microbial biodegradable poly(3-hydroxybutyrate)/organoclay nanocomposite. Journal of Materials Science Letters, 22 (4), 299-302.

Mansur, H. S., Sadahira, C. M., Souza, A. N., & Mansur, Al A. P. (2008). FTIR spectroscopy characterization of poly(vinyl alcohol) hydrogel with different hydrolysis degree and chemically crosslinked with glutaraldehyde. Materials Science and Engineering: C, 28 (4), 539-548.

Mergaert, J., Webb, A., Anderson, C., Wouters, A., & Swings, J. (1993). Microbial degradation of poly(3-hydroxybutyrate) and poly(3-hydroxybutyrate-co-3-hydroxyvalerate) in soils. Applied and Environmental Microbiology, 59(10), 3233-3238.

Mousavioun, P., George, G. A, & Doherty, W. O. S. (2012). Environmental degradation of lignin/poly(hydroxybutyrate) blends. Polymer Degradation and Stability, 97 (7), 1114-1122.

Nasar, G., Khan, M. S., & Khalil, U. (2009). Structural study of PVA composites with inorganic salts by X-ray diffraction. Journal of the Pakistan Materials Society, 3,67-70.

Nicho, M. E., & Hu, H. (2000). Fourier transform infrared spectroscopy studies of polypyrrole composite coatings. Solar Energy Materials and Solar Cells, 63 (4), 423-435.

Nichols, P. D., Michael Henson, J., Guckert, J. B., Nivens, D. E., & White, David C. (1985). Fourier transform-infrared spectroscopic methods for microbial ecology: analysis of bacteria, bacteri-polymer mixtures and biofilms. Journal of Microbiological Methods, 4 (2), 79-94.

Nikolova, A., & Schnabel, R. (2014). Rheological investigations of poly (hydroxybutyrate) and poly (ethylene oxide) solutions and their mixtures. Journal of

Chemical Technology and Metallurgy, 49 (4), 494-498.

Pachekoski, W. M., Agnelli, J. A. M., & Belem, L. P. (2009b). Thermal, mechanical and morphological properties of poly(hydroxybutyrate) and polypropylene blends after processing. Materials Research, 12 (2), 159-164.

Pal, M., & Gautam, J. (2013). Effects of inorganic nanofillers on the thermal degradation and UV-absorbance properties of polyvinyl acetate. Journal of Thermal Analysis and Calorimetry, 111 (1), 689-701.

Park, S. H., Lim, S. T., Shin, T. K., Choi, H. J., & Jhon, M. S. (2001). Viscoelasticity of biodegradable polymer blends of poly(3-hydroxybutyrate) and poly(ethylene oxide). Polymer, 42 (13), 5737-5742.

Ramachander, T. V. N., Rohini, D., Belhekar, A., & Rawal, S. K. (2002). Synthesis of PHB by recombinant E. coli harboring an approximately 5 kb genomic DNA fragment from Streptomyces aureofaciens NRRL 2209. International Journal of Biological Macromolecules, 31 (1–3), 63-69.

Saad, Gamal R., & Seliger, Hartmut. (2004). Biodegradable copolymers based on bacterial Poly((R)-3-hydroxybutyrate): thermal and mechanical properties and biodegradation behaviour. Polymer Degradation and Stability, 83 (1), 101-110.

Sato, H., Murakami, R., Zhang, J ,.Ozaki, Y., Mori, K., Takahashi, I., Terauchi, H., & Noda, I. (2006). X-ray diffraction and infrared spectroscopy studies on crystal and lamellar structure and cho hydrogen bonding of biodegradable poly(hydroxyalkanoate). Macromolecular Research, 14(4), 408-415.

Selvasekarapandian, S., Baskaran, R., & Hema, M. (2005). Complex AC impedance, transference number and vibrational spectroscopy studies of proton conducting PVAc–NH4SCN polymer electrolytes. Physica B: Condensed Matter, 357 (3–4), 412-419.

Selvasekarapandian, S., Baskaran, R., Kamishima, O., Kawamura, J., & Hattori, T. (2006). Laser Raman and FTIR studies on Li+ interaction in PVAc–LiClO4 polymer electrolytes. Spectrochimica Acta Part A: Molecular and Biomolecular Spectroscopy,

65 (5), 1234-1240.

Shah, K. (2012). FTIR analysis of polyhydroxyalkanoates by a locally isolated novel Bacillus sp. AS 3-2 from soil of Kadi region, North Gujarat, India. Journal of Biochemical Technology, 3(4), 380-383.

Shawaphun, S., Buasuwan1, S., & Manangan, T. (2011). Structural Modification of Poly-3-Hydroxyalkanoate Produced from A.latus. Pure and Applied Chemistry International Conference 2011, Januray 5-7, 886-889.

Sivalingam, G., Karthik, R., & Madras, G. (2004). Blends of poly(ε-caprolactone) and poly(vinyl acetate): mechanical properties and thermal degradation. Polymer Degradation and Stability, 84 (2), 345-351.

Sivalingam, G., & Madras, G. (2004). Thermal degradation of ternary blends of poly (ε-caprolactone)/poly(vinyl acetate)/poly(vinyl chloride). Journal of Applied Polymer Science, 93 (3), 1378-1383.

Sombatmankhong, K., Suwantong, O., Waleetorncheepsawat, S., & Supaphol, P. (2006). Electrospun fiber mats of poly(3-hydroxybutyrate), poly(3-hydroxybutyrate-co-3-hydroxyvalerate), and their blends. Journal of Polymer Science Part B: Polymer Physics, 44 (19), 2923-2933.

Song, M., & Long, F. (1991). Miscibility in blends of poly(vinyl acetate) with poly(methyl methacrylate) studied by FTIR and DSC. European Polymer Journal, 27 (9), 983-986.

Srilalitha, S., Jayaveera, K., & Madhvendra, S. (2011). Synthesis & Studies of Differential Scanning Calorimetry, Scanning Electron Microscopy and Mechanical Properties of Biodegrade Poly(β-Hydroxy Butyrate), Its Applications and A Comparative Study With PolyPropylene. International Refereed Journal of Engineering and Science 2 (6), 30-32.

Verhoogt, H., Ramsay, B. A., & Favis, B. D. (1994). Polymer blends containing poly(3-hydroxyalkanoate)s. Polymer, 35 (24), 5155-5169.

Wada, Y., Seko, N., Nagasawa, N., Tamada, M., Kasuya, K.-i., & Mitomo, H. (2007). Biodegradability of poly(3-hydroxybutyrate) film grafted with vinyl acetate: Effect of grafting and saponification. Radiation Physics and Chemistry,76 (6), 1075-1083.

Wang, L., Zhu, W., Wang, X., Chen, X., Chen, G.-Q., & Xu, Kaitian. (2008). Processability modifications of poly(3-hydroxybutyrate) by plasticizing, blending, and stabilizing. Journal of Applied Polymer Science, 107 (1), 166-173.

Wei, Q., & Huang, F. (2010). Preparation and Properties of Organic/inorganic Hybrid Nanofibres. Fibres & Textiles in Eastern Europe, 18 (1), 21 -23.

Wu, N., Wang, J., Wei, Q., Cai, Y., & Lu, B. (2009). Morphology, thermal and mechanical properties of PVAc/TiO2 hybrid nanofibers. e-Polymers, 9 (1), 1803-1810.

Xu, S., Luo, R., Wu, L., Xu, K., & Chen, G.-Q. (2006). Blending and characterizations of microbial poly(3-hydroxybutyrate) with dendrimers. Journal of Applied Polymer Science, 102 (4), 3782-3790.

Zaikov, G.E. (2005). Chemistry Of Polysaccharides: Taylor & Francis Group.

Zhang, L., Deng, X., Zhao, S., & Huang, Z . (1997b). Biodegradable polymer blends of poly(3-hydroxybutyrate) and starch acetate. Polymer International, 44 (1), 104-110.

Zhang, M. (2011). Development of polyhydroxybutyrate based blends for compostable packaging. (Unpublished Doctoral thesis). Loughborough University's Institutional Repository, UK.

Zhu, C., Nomura, C. T., Perrotta, J. A., Stipanovic, A. J., & Nakas, J. P. (2010). Production and characterization of poly-3-hydroxybutyrate from biodiesel-glycerol by Burkholderia cepacia ATCC 17759. Biotechnology Progress, 26 (2), 424-430.

Zuber, M., Zia, K. M., Bhatti, I. A., Jamil, T., Fazal ur, R., & Rizwan, A. (2012). Modification of cellulosic fabric using polyvinyl alcohol, part-II: Colorfastness properties. Carbohydrate Polymers, 87 (4), 2439-2446.

Zulfiqar, S., & Ahmad, S. (2001). Thermal degradation of blends of PVAC with polysiloxane— II. Polymer Degradation and Stability, 71 (2), 299-304.